

Univerzita Karlova v Praze
Přírodovědecká fakulta

Studijní program: Geologie



RNDr. Zdeňka Čermáková, G.G. (GIA)

Mineralogická analýza historických maleb

Disertační práce

Školitel: Mgr. David Hradil, Ph.D.

Konzultanti: Dr. RNDr. Petr Bezdička, Ing. Silvie Švarcová, Ph.D.

Praha, 2014

University of Charles in Prague
Faculty of Science

Study Programme: Geology



RNDr. Zdeňka Čermáková, G.G. (GIA)

Mineralogical Analysis of Historical Paintings

Dissertation

Supervisor: Mgr. David Hradil, Ph.D.

Co-Supervisors: Dr. RNDr. Petr Bezdička, Ing. Silvie Švarcová, Ph.D.

Praha, 2014

Prohlášení:

Prohlašuji, že jsem závěrečnou práci zpracovala samostatně a že jsem uvedla všechny použité informační zdroje a literaturu. Tato práce ani její podstatná část nebyla předložena k získání jiného nebo stejného akademického titulu.

V Praze, 17. 12. 2014

Podpis

ACKNOWLEDGEMENTS

This Ph.D. research has been supported by Charles University Grant Agency, project No. 632212, Czech Science Foundation, projects No. P103/12/2211 and No. 14-22984S, NAKI project of Ministry of Culture of the Czech Republic No. DF12P01OVV048 and RVO 61388980.

First of all, I would like to express my gratitude to my supervisor Dr. David Hradil for his expert guidance, insightful and constructive comments throughout my Ph.D. studies and for fruitful discussions about the performed research. My deepest thanks belong also to my co-supervisors, Dr. Petr Bezdička and Dr. Silvie Švarcová. Dr. Bezdička is an expert in X-ray diffraction measurements and provided valuable insight into his field of research. Silvie helped me with her advice and expert guidance in all matters chemical, shared with me her experiences with Ph.D. studies and she has been a great friend and colleague.

I would like to thank all my other colleagues from the ALMA Laboratory for fruitful cooperation, namely RNDr. Janka Hradilová for her expertise in optical microscopy and painting technique, Mgr. Vlasta Vašutová and Mgr. Pavla Bauerová for their versatile cooperation in sample preparation and experimental work, enthusiasm and friendship as well as Mgr. Veronika Košařová for her friendship and discussions about Raman spectra.

My gratitude also belongs to all who helped me with the measurements of vibrational spectroscopies: Doc. Ivan Němec, Dr. Irena Matulková, Prof. Jan Jehlička, Dr. Kateřina Osterrothová, Dr. Adam Culka (Faculty of Science, Charles University in Prague), Mgr. Eva Dytrychová, Mgr. Jakub Havlín, Dr. Petra Lesniaková (Faculty of Restoration, University of Pardubice), Ing. Zlata Vrátníčková (Polymer Institute Brno), Jitka Večerníková (Institute of Inorganic Chemistry, AS CR) and RNDr. Ján Pásztor (Nicolet CZ). I would like to further acknowledge Dr. Kamil Lang (IIC AS CR) and Mgr. Petr Henke (Faculty of Science, Charles University in Prague) for their help with UV/VIS spectrophotometric measurements. My thanks belong also to Dr. Adriana Lančok (IIC AS CR) for measurement and data interpretation of Mössbauer spectroscopy and Petr Vorm (IIC AS CR) for analyses of solutions for synthesis of vivianite. The performance of model relining, a conservation technique, has been made possible thanks to restorer and painter MgA. Tomáš Tichý; Ing. Eva Večerníková and Dr. Jiří Plocek are acknowledged for lending the necessary equipment. Thanks belong also to Mgr. Jan Blažek (IITA AS CR) for performing the analysis of image histograms.

The presented studies could not be made without mineralogical samples and micro-samples of works of art. I would like to express my thanks to Mgr. Dalibor Velebil (National Museum in Prague), Andreas Massanek, Dipl.-Min. (TU Bergakademie Freiberg), RNDr. Vladimír Šrein, CSc. (Czech Geological Survey) and Mgr. Viktor Goliáš, Ph.D. (Faculty of Science, Charles University in Prague) for providing the mineralogical samples. All the restorers who cooperated with ALMA Laboratory, provided micro-samples of works of art and valuable information regarding the studied works are gratefully acknowledged.

I would like to thank all my friends at the Institute of Inorganic Chemistry of the AS CR, especially Dr. Petr Svora, Ing. Eva Plížingrová, Dr. Mariana Klementová, Mgr. Monika Palkovská, Lenka Volfová and restorer and painter Mgr. Sylwia Pawełkiewicz for their pleasant company and insightful scientific remarks.

Finally, my greatest thanks belong to my parents, who have always supported me, loved me and believed in me, to my whole family for being there for me, and especially to my loving husband Petr, who has always been my rock.

ABSTRAKT

Historická malířská díla mají velmi komplexní vnitřní strukturu. Dobová malířská technika vedla k použití podkladové vrstvy, několika vrstev podmaleb a svrchní malby, která byla následně pro vyšší odolnost proti vnějším vlivům přelakována. Každá barevná vrstva obsahuje barvivo či pigment (nebo jejich směs) v kombinaci s organickým pojivem. Pigmenty byly v průběhu historie často tvořeny minerály, ať už byly získávány z přírodních ložisek, nebo připravovány uměle. V těchto heterogenních vrstvách s anorganickými i organickými komponentami pak může docházet k nežádoucím degradačním změnám, ať už vlivem procesů probíhajících přímo v barevné vrstvě, nebo vlivem vnějších podmínek. Mineralogický přístup, který se zaměřuje především na strukturu studovaných pigmentů, může napomoci k objasnění probíhajících procesů, stanovení podmínek vedoucích k degradaci a identifikaci původních/degradovaných fází. Dále je přínosem pro mikroanalytické určení pigmentů přítomných v drobných mikrovzorcích získaných z malířských děl, a může přispět jak ke studiu jejich provenience a autorství, tak ke zjištění regionální provenience použitých minerálních pigmentů.

Předkládaná práce je zaměřena na mikroanalýzu vzácných minerálních pigmentů vivianitu, přírodně ozářeného fluoritu – antozonitu a krokoitu a zabývá se také jejich významem pro určení provenience díla; mikroanalýza barevné vrstvy je dále rozvinuta na široké skupině měďnatých pigmentů. Práce se rovněž věnuje degradačním procesům způsobených jak vnitřními, tak vnějšími vlivy na příkladu hoganitu, vivianitu a auripigmentu.

Strukturní studium mineralogických vzorků modrého vivianitu ($\text{Fe}_3(\text{PO}_4)_2 \cdot 8\text{H}_2\text{O}$) a jeho přírodně se vyskytujících oxidačně degradačních produktů vedly k aplikaci výsledků na mikrovzorky – bylo zjištěno, že vhodná kombinace strukturních metod pro identifikaci vivianitu v barevné vrstvě je rtg. mikrodifrakce s mikroinfračervenou spektroskopií v uspořádání zeslabení úplného odrazu (mikro-ATR). Vivianit patří mezi vzácnější pigmenty; byl používán jen některými autory, např. v holandské malbě 17. a 18. století. Vivianit byl identifikován v sedmi obrazech Jeana George de Hamiltona, což byl jeden z faktorů prokazujících jeho autorství. Prvkové složení a morfologie vivianitového pigmentu ve srovnání s mineralogickými a modelovými vzorky naznačilo jeho sedimentární původ. Studium mineralogických vzorků antozonitu (silně přírodně ozářený tmavě fialový až černý CaF_2) ukázalo, že čím silnější je poškození jeho struktury, tím větší je rozšíření linií na difrakčním záznamu a tím tmavší je jeho barva. Naopak uváděné zvětšení základní buňky není přímo úměrné míře poškození. Práce představuje charakteristické Ramanovo spektrum antozonitu, díky kterému může být snadno detekován při mikroanalýze, jak ukázalo měření mikrovzorku oltářního obrazu z Vlašského dvora v Kutné Hoře z roku 1497. Vzhledem k zřejmě omezené době historické těžby může přítomnost antozonitu potvrdit předpokládanou dobu vzniku studovaného díla. Datace může být podpořena rovněž identifikací extrémně vzácného žlutooranžového pigmentu krokoitu (PbCrO_4). Byl nalezen v unikátních nástěnných malbách v kostele sv. Havla v Kuřívodech, a přispěl tak k jejich vročení do konce 13. století. Měďnaté pigmenty tvoří širokou skupinu chemicky podobných fází. V předkládané práci byla rozvinuta jejich mikroanalýza v barevné vrstvě vedoucí k identifikaci jak minerálních pigmentů, tak pigmentů na bázi měďnek.

Degradaci v rámci chemického složení barevné vrstvy přiblížily modelové experimenty s neutrální měďenkou (mineralogicky hoganit), která ztrácí v kombinaci s proteinovými pojivy svoji strukturu. Její detekce ve vrstvě je dále ztížena častou přítomností silně difraktujících pigmentů. K degradaci vlivem vnějších podmínek dochází u vivianitu. Experimenty naznačily, že vivianit je citlivý jak při vystavení zvýšeným teplotám již od 70°C (studováno vysokoteplotní rtg. difrakcí a Mössbauerovou spektroskopií, změna barevnosti ověřena při provedení modelové rentoaláže – restaurátorského zásahu, při kterém je na staré plátno obrazu zespod nažehleno plátno nové), tak při vystavení zvýšené vlhkosti. Na závěr byl teoreticky navrhnout degradační proces auripigmentu v nástěnných malbách, který bude v následujícím výzkumu experimentálně ověřen.

ABSTRACT

Historical painted works of art have a very complex inner structure. The period painting technique led to the execution of a ground layer followed by several layers of underpainting and a top paint layer, over which a layer of glaze has been applied to increase the resistance to external wear. Each of these colour layers is composed of a dye or a pigment (or their mixture) bound by organic binder. Throughout the history, pigments were commonly prepared from minerals, either extracted from natural deposits or created artificially. In these heterogeneous layers containing both inorganic and organic components, undesirable degradation changes either driven by processes taking place directly in the colour layer or influenced by external agents may occur. Mineralogical approach, which focuses primarily on the structure of studied pigments, helps in the clarification of the occurring processes, in the determination of conditions leading to degradation as well as in the identification of original/degradation phases. Furthermore, it can be profitably applied in the micro-analysis of mineral pigments present in tiny micro-samples obtained from works of art, contributes to the artwork's provenance/authorship studies and the determination of regional provenance of the employed mineral pigments.

This Ph.D. thesis focuses on the micro-analysis of rare mineral pigments vivianite, naturally irradiated fluorite – antozonite and crocoite, and also deals with their significance for provenance studies; the micro-analysis has been also performed on a large group of copper-based pigments. In addition, the thesis deals with the degradation processes caused by internal/external agents with special attention to hoganite, vivianite and orpiment.

A structural study of mineralogical samples of blue vivianite ($\text{Fe}_3(\text{PO}_4)_2 \cdot 8\text{H}_2\text{O}$) and its naturally occurring degradation products led to the application of the results on micro-samples – a suitable combination of structural methods for the identification of vivianite in colour layer was found to be X-ray micro-diffraction with micro-infrared spectroscopy in micro-attenuated total reflectance mode. Vivianite is rare pigment and has been used only by certain authors, e.g. in the Dutch painting of the 17th and 18th century. This thesis describes the identification of vivianite in seven paintings by Jean George de Hamilton, which was one of the factors confirming his authorship. The comparison of elemental composition and grain morphology of vivianite pigment with mineralogical and model samples indicated its sedimentary origin. The study of mineralogical samples of antozonite (heavily naturally irradiated dark violet to black CaF_2) showed that the higher is its structural damage, the broader are the diffraction lines in its diffraction pattern and the darker is its colour. On the other hand, the reported increase of the unit cell volume is not in direct proportion to the level of structural damage. A characteristic Raman spectrum of antozonite is presented thanks to which it can be easily micro-analytically detected, as shown on micro-samples of the altar painting from Italian Court in Kutná Hora created in 1497. Taking into account the limited period of antozonite's extraction, its presence may prove the expected date of execution of the studied work of art. The dating may be supported also by the identification of extremely rare yellow-orange pigment crocoite (PbCrO_4). It was found in unique wall paintings in the church of St. Gallus in Kuřívody, thus contributing to their dating to the end of the 13th century. Copper-based pigments form a large group of chemically similar phases. In this thesis, their micro-analysis in paint layer leading to the identification of both mineral-type and verdigris-type pigments has been elaborated.

Degradation caused by internal agents, i.e. the chemical composition of the colour layer, has been studied using model experiments with neutral verdigris (mineralogically hoganite), which loses its structure in combination with proteinaceous binders. Its detection in the colour layer has been further complicated by frequent presence of highly diffracting pigments. The degradation caused by external agents has been studied on vivianite. The experiments showed that vivianite is prone to degradation both under increased temperatures from 70°C on (studied by high-temperature X-ray diffraction and Mössbauer spectroscopy, the colour change has been verified on model relining – a restoration/conservation treatment during which a new canvas is ironed to the back of the painting's old one) and under increased humidity. Finally, a degradation pathway of orpiment in wall paintings has been theoretically proposed; it will be experimentally verified in the following research.

TABLE OF CONTENTS

1. INTRODUCTION	1
1.1 MOTIVATION	1
1.2 AIMS OF THE WORK	2
2. STATE OF THE ART	3
2.1 MICRO-ANALYSIS OF PAINT LAYERS	3
2.2 MINERALOGICAL APPROACH TO ANALYSIS	6
2.3 MINERAL PIGMENTS IN FINE ART – BRIEF OVERVIEW	7
2.4 PIGMENTS SELECTED FOR THIS STUDY	9
3. EXPERIMENTAL	11
3.1 MINERALOGICAL SAMPLES	11
3.2 ARTWORKS' MICRO-SAMPLES	12
3.3 MODEL SAMPLES	15
3.3.1 HOGANITE MODEL SAMPLES	15
3.3.2 SYNTHESIS OF VIVIANITE	15
3.3.3 VIVIANITE MODEL SAMPLES	16
3.4 MODEL EXPERIMENTS WITH VIVIANITE	17
3.4.1 HIGH TEMPERATURE X-RAY DIFFRACTION EXPERIMENT (IN SITU)	17
3.4.2 TEMPERATURE EXPERIMENTS (EX SITU)	17
3.4.3 CONSERVATION TECHNIQUE – RELINING	18
3.4.4 HUMIDITY EXPERIMENTS	18
3.5 ANALYTICAL METHODS	18
3.5.1 OPTICAL MICROSCOPY, PHOTOGRAPHY	18
3.5.2 PORTABLE X-RAY FLUORESCENCE	19
3.5.3 SCANNING ELECTRON MICROSCOPY – ENERGY DISPERSIVE SPECTROSCOPY	19
3.5.4 X-RAY DIFFRACTION AND X-RAY MICRO-DIFFRACTION	19
3.5.5 RAMAN SPECTROSCOPY	20
3.5.6 FOURIER-TRANSFORM INFRARED SPECTROSCOPY	21
3.5.7 MÖSSBAUER SPECTROSCOPY	22
3.5.8 UV-VIS SPECTROPHOTOMETRY AND ANALYSIS OF IMAGE HISTOGRAMS	22
4. RESULTS AND DISCUSSION	24
4.1 MICRO-ANALYSIS OF MINERAL PIGMENTS AND THEIR PROVENANCE/AUTHORSHIP STUDIES	24
4.1.1 VIVIANITE	24
4.1.2 NATURALLY IRRADIATED FLUORITE	28
4.1.3 CROCOITE	32
4.1.4 COPPER-BASED PIGMENTS	33

4.2 PIGMENT DEGRADATION	38
4.2.1 CAUSED BY INTERNAL AGENTS	38
4.2.2 CAUSED BY EXTERNAL AGENTS	39
5. CONCLUSIONS	45
<hr/>	
6. REFERENCES	46
<hr/>	
APPENDIX A – PUBLISHED PAPERS	
<hr/>	

1. INTRODUCTION

1.1 MOTIVATION

Mineralogy and cultural heritage seem to belong to very different worlds. Mineralogy implies field trips under rash conditions in remote mountain terrain or deep down in the mine shafts, while cultural heritage evokes the silence of galleries and museums, contemplation of pieces of art. Nevertheless, in the historical paintings, these two fields of study meet – in the usage of a colourful palette of minerals in the process of artistic expression.

Historical painted works of art have a very complex structure. The paints were prepared from pigment(s)/dye(s) and organic binders like egg, oil or skin glue, resulting in a complex mixture with the desired colour and covering power. The creation of a specific hue or the employed painting technique often required application of paints in several consecutive layers. Since prehistoric times, paints have been prepared from natural minerals; they were mined and extracted, but some of them have also been prepared artificially, like green copper pigment verdigris (mineralogically hoganite), which was manufactured by corrosion of copper plates exposed to wine vinegar fumes. All these organic and inorganic components are present in paint layers for several tens, hundreds or even thousands of years, sometimes in much less-than-ideal conditions of exhibition or storage. It may result in slight to severe degradation, which usually starts with the organic components; their products may have degradative effect on the inorganic compounds, and even some of the minerals are not stable in time (like vivianite, a hydrated ferrous phosphate). The degradation may be accompanied by colour change, which highlights the occurring processes; in some cases, the degradation changes internal characteristics, but the colour of the paint remains the same. These changes may be specified by mineralogical approach, which focuses on crystal structure of the studied materials, the influence of external conditions and internal types of structural degradation. In addition, it contributes to the differentiation of the original pigments and their degradation products in the paint layer, which is essential for art-historical studies – interpretation of the degradation phase as the intentionally used original one may lead to erroneous conclusions.

The information gained through mineralogical study of pigments may further serve for correct identification of mineral phases in complex mixtures present in the paint layers. The study is complicated by the nature of the samples obtainable from the works of art – since the impact on the artwork needs to be kept to minimum, the samples are tiny with dimensions only rarely exceeding 1 mm. Consequently, the applicability of standard procedures is problematic and the limitations of the methods in micro-scale have to be carefully evaluated. Structural micro-analytical methods may help in discerning e.g. copper-based pigments like azurite, malachite, verdigris, brochantite or posnjakite, which is challenging due to their highly similar elemental composition.

Identification of certain pigments and their characteristics may lead, if interpreted in appropriate context, to indications regarding the authorship of the artwork, its provenance or date of creation. Certain painters/workshops preferred certain types of pigments, or these pigments were used regionally/in specific period of time. Pigments suitable for such

studies encompass clay-based pigments, or rare pigments like naturally irradiated fluorite (antozonite), vivianite or crocoite. The provenance studies may focus on the artworks, or the pigment itself. It is well-known that the same minerals are often formed under different geological conditions, with different morphology, different minor/trace element composition, or slightly different structure. Together with profound historical research regarding the extraction of pigments and a thorough analysis of natural samples from possible localities, the research may lead to specification of the deposit of the pigment. However, one must take into account the thriving historic market with pigments; an indication of the pigment's provenance does not necessarily imply similar provenance of the artwork.

The mineralogical field of study in cultural heritage is very wide; this dissertation presents some of the problems regarding painted works of art that have been tackled during this Ph.D. research.

1.2 AIMS OF THE WORK

The first aim of this work was to study historical mineral painting pigments important for the provenance and authorship studies, either in a geological sense (the place of origin/type of locality of the mineral pigment), or in an art-historical one (indications of affiliation with certain geographical areas or workshops). Consequently, following rare mineral pigments, which are generally highly suitable for this purpose, were studied: vivianite, naturally irradiated fluorite and crocoite. The group of clay minerals, even though also very important in this respect, has not been included in this study, since they represent a very wide topic and would exceed the scope of this thesis.

Another aim of the work closely interconnected with the first one was the performance of correct micro-analysis of the above-stated pigments in the tiny micro-samples obtained from works of art. It was further complemented by the study of micro-analytical evidence of copper-based pigments, whose chemical similitude represents an analytical challenge.

Finally, the subjects of study encompassed also pigment degradation. The aim was to clarify the degradation processes of hoganite, to evaluate the influence of external agents on the degradation of vivianite, and to suggest the degradation pathways of orpiment.

2. STATE OF THE ART

2.1 MICRO-ANALYSIS OF PAINT LAYERS

A work of art commonly has an intricate inner structure. In the past, the creation of a painting was as much about art as about knowing how to execute it correctly. It was necessary to know the painting technique. This technique has changed and evolved in relation to period and geographic location. Nevertheless, regarding the European art in the 13th to 18th century which covers the studied paintings in this thesis, certain general remarks can be made.

First of all, on the support of choice (wood, canvas etc.) covered by an organic layer of insulation, a ground layer was applied. Some of the commonly encountered materials forming ground layers are earths, chalk or gypsum. The ground layer served mainly for the smoothing of the support and had to be relatively thick (ca 100 to 300 μm). It is also much more pleasing to paint on it compared to the support itself, and helps in the adhesion of the following layers. Then, another organic layer of insulation was usually applied, sealing the ground layer and preventing its grains from entering the following layers. After that, the preparatory drawing has been performed, followed by application of underpainting which gave a desired tint to the final paint layers observable on the surface of the painting. These layers are much thinner than the ground one, usually in order of several tens of micrometres. Finally, the painting has been varnished so it would be more resistant to outer wear. For various reasons, other paint layers may be applied on the already varnished painting – change of taste led to partial or complete overpainting, or the painting has been retouched (Hradilová, 2013).

To study a work of art, its materials and its painting technique in depth, it is necessary to study its micro-samples, which reveal its inner structure. The sampling is often performed during conservation/restoration stage using small scalpels and needles. If the sampling is performed correctly, the resulting micro-sample contains all the layers present in the painting, is tiny in order to preserve as much of the original painting as possible, and is representative.

To study the stratigraphy, i.e. the layout of the layers, micro-samples are embedded in synthetic resin and ground to obtain cross-sections. They reveal that each paint layer is composed of pigment/dye (or their mixture) and an organic binder. The hundreds of years the materials spend in such complex mixtures in sometimes less-than-ideal outer conditions lead to possible material deterioration, degradation, colour changes and creation of phases not originally present in the painting. The cross-sections are tiny, extremely heterogeneous and should not be destroyed during the course of the analysis as they are unique and scarce. Samples of such nature represent a challenge for analytical approach and push the analytical limits of respective instrumental methods.

The first step in the study of micro-samples is their visual observation under optical microscope. A thorough study at this stage is vital. It differentiates stratigraphy of the layers and prevents misinterpretation of the data obtained by further analyses, colour description suggests present pigments or their potential degradation, and enables comparative studies

of the painting technique. The observations under visible light are supported by the ones under UV light – the luminescence behaviour provides further characterisation.

Optical microscopy is often followed by scanning electron microscopy. If the analysis takes place in low-vacuum mode, it is not necessary to apply conductive coating on the sample, since the charge is eliminated on air molecules present in the chamber. The back-scattered electron (BSE) mode displays in black and white scale the average atomic weight of the analysed areas – the heavier the elements, the lighter is the area. Scanning electron microscopy – energy dispersive spectroscopy (SEM-EDS) enables the elemental study of paint layers as well as of individual grains, which may lead to pigment determination. However, optical characteristics and elemental composition may not be sufficient for unambiguous identification of the material, therefore, further methods should be employed.

Optical and scanning electron microscopies are relatively common in the study of micro-samples of cultural heritage objects. Vibrational spectroscopies – infrared (IR) and Raman – are methods that are not that often employed, but are becoming increasingly popular, which is documented by growing number of spectroscopic studies (Perez-Rodriguez et al., 2014; Pitarch et al., 2014; Pięta et al., 2014; Rodríguez et al., 2010; De Benedetto et al., 2013). They both reflect vibrational modes of molecules and describe chemical and structural nature of the studied material. Certain vibrations may be active in both Raman and infrared spectroscopies; however, the selection rules of respective methods are different. While infrared spectroscopy relies on absorption of mid-IR wavelengths based on the electric dipole-mediated transition between vibrational energy levels, Raman spectroscopy represents two-photon inelastic light scattering which occurs due to Raman polarisability of the molecule (Larkin, 2011). The resulting spectra are characteristic; identification is based on the comparison of spectra of analysed substances with the reference ones.

Infrared spectroscopy is a versatile method and can be used for identification of both organic and inorganic materials, regardless of their crystalline or amorphous nature. The so-called standard mode of IR analysis is the transmission one; however, in the study of cross-sections embedded in resin, the modes of choice are reflection or attenuated total reflectance (ATR) ones, ideally micro-ATR. The microscopes with reflection mode are the most common. However, such analyses have their disadvantages. The first one is the distortions of the spectra. Some of them represent a predictable physical response and as such may be removed from the spectra by mathematical corrections (Lichvár et al., 2002). However, since the micro-samples are less-than-ideal (e.g. not completely flat, not enough reflective), other unpredictable distortions may occur and the interpretation of the data and comparison of the spectra with standard transmission ones may prove to be difficult. Another problem is space resolution, which is – in micro-analysis – a critical issue. Micro-infrared spectroscopy in reflection mode can produce good results from 20x20 μm on; smaller areas up to 10x10 μm may be analysed, but the signal is low and the spectrum is often uninterpretable (Prati et al., 2010). Analysis of larger areas results in combination of signal from different materials, which further complicates the identification. On the other hand, micro-ATR mode has better resolution as well as noise (Mazzeo et al., 2007); furthermore, spectra collected in micro-ATR mode are often very similar to the transmission ones. However, micro-ATR micro-spectroscopes do not belong, so far, among common laboratories' instrumentation. An interesting aspect of the analysis is also represented by the optics of the micro(spectro)scope – since not only visible, but also infrared radiation has

to pass through, the image of the micro-sample is of relatively low quality, and sometimes correct location of the analysis area poses a challenge. To know what exactly we analyse is vital for interpretation of the results.

Compared to infrared micro-spectroscopy, Raman micro-spectroscopy has an excellent spatial resolution, which reaches 1 μm . On the other hand, measurements may be hindered by the presence of undesirable fluorescence, which may completely prevent the identification of the studied material, but can be reduced by suitable choice of excitation wavelength or objective with higher magnification (Correia et al., 2007; Cristini et al., 2010). During the analysis, the material is excited by laser; consequently, potential thermal degradation is a serious issue and the laser power has to be carefully monitored and appropriately adjusted. Smith et al. (2001) reported an erroneous identification of plattnerite in Boticelli's Trionfo d'Amore by Andalò et al. (2001), which was in fact created by laser-induced degradation of another lead-based material, most probably massicot. Mattei et al. (2008) pointed out potential laser-induced degradation of azurite grains smaller than 25 μm . Such degradation results in formation of black copper oxide tenorite and may lead to incorrect interpretation of the actual state of the studied work of art.

Various excitation lasers are available, most commonly 532 (or 514.5) nm, 633 nm, and 780 (or 785) nm. The interpretation of the resulting spectra has to be performed with care; spectra collected using different excitation wavelengths may, to a certain extent, vary. Furthermore, some materials do not provide sufficient Raman scattering to be visible in the spectrum, especially in mixture with very good Raman scatterers. This has been recently reported by Košařová et al. (2013) in case of analysis of Fe-rich earths, which resulted only in the spectrum of hematite, even though clay minerals formed major part of the material. Still, if performed and interpreted correctly, Raman micro-spectroscopy represents a powerful micro-analytical tool able to characterise individual grains of pigments in the paint layers.

An excellent method for structural characterisation of crystalline substances is powder X-ray diffraction (XRD), for micro-analytical purposes in its micro-configuration. X-ray diffraction is based on interaction of X-rays with the studied material resulting in a characteristic diffraction pattern, which may be described as the intensity of X-ray scattering as a function of scattering direction (Zachariassen, 2004). The essential constituents of the instrumentation enabling X-ray diffraction measurements in micro-scale are capillaries/collimators that reduce the X-ray beam size and sufficiently efficient detectors substituting for the relatively weak signal obtained from the small irradiated area. One of the configurations used for the analysis of paint layers employ glass mono-capillary with 100 μm diameter collimating the X-ray beam and a multichannel detector. In this case, the irradiated area of the sample equals to an ellipse with a constant width of 142 μm , because the incident beam is slightly divergent to the monocapillary aperture. The length of the ellipse depends on the angle of incidence of the X-ray beam, i.e. on the 2 Theta angle range that is being measured (Švarcová et al., 2010). Usually, the best results are obtained with ground layers, which are thick enough to get a signal not interfered by adjacent layers or the embedding resin. The resin is amorphous, but it creates an undesirable "bump" in the pattern, which may result in overlap with characteristic diffraction lines. Ideally, the analysis is performed on micro-samples before their embedment into resin, assuming the layer of interest is sufficiently exposed. The benefits of micro-XRD lie in its robustness – the diffraction patterns' reference database is extensive and the analysed crystalline materials always produce signal (if present in a sufficient amount, usually around several wt. %

depending on the X-ray absorption of the material) (Švarcová et al., 2010; Nel et al., 2006). On the other hand, micro-XRD has certain limitations – correct analysis of the present phase can be performed only when sufficient amount of its crystallites is present in the small area that is being irradiated. Another important factor influencing the analysis is the particle size. Švarcová et al. (2010) tested the X-ray micro-diffraction analysis on diamond crystals with different particle size and found out that the maximum grain size for reliable identification is 20-30 µm. Since the paint layers in micro-samples of works of art cannot be ground for the analysis, the coarseness of certain painting materials may hinder the results. The small size of the irradiated area also results in a worsened signal to noise ratio, and together with the decreased detection limit caused by capillary-collimated parallel X-ray beam result in a substantial prolongation of the measurement time (Nel et al., 2006; Miguel et al., 2009).

Since micro-XRD is a bulk analysis, it commonly contains superimposed diffraction patterns of several crystalline substances. However, this usually does not represent a problem, since – especially in combination with SEM-EDS elemental analysis – numerous diffraction patterns can be assigned.

2.2 MINERALOGICAL APPROACH TO ANALYSIS

In practice, the majority of studied micro-samples are analysed only by optical microscopy, sometimes also by SEM-EDS. They are powerful tools, but in many cases, following structural analysis by vibrational spectroscopies or X-ray micro-diffraction is required for unambiguous identification of studied materials. The analyses of micro-samples of cultural heritage are commonly performed by analysts with chemical technology background. Since a large amount of historic pigments are natural minerals, the best results are usually achieved in cooperation with mineralogists. Such situation is, however, still scarce.

Mineralogical approach puts an emphasis on work with structural information. Mineralogy studies polymorphism, i.e. different structure of minerals with similar elemental composition, deals with natural degradation processes of minerals accompanied by structural changes, and relates structural/elemental characteristics of minerals with their respective geological origin.

An example of mineralogical approach is the study of clay minerals. They form major part of ground layers made from earths; as they cannot be distinguished based on their elemental composition, their study has been, for long, neglected. This has been also accentuated by general interest in upper paint layers in contrast to ground layers, because the grounds were often prepared by artisans, not by the artist himself. However, the composition and application technique of ground layers may provide indication of both period and provenance of the artwork's creation. Careful structural analysis by X-ray diffraction can differentiate not only the present clay minerals, but also their more specific characteristics, such as level of crystallinity. The crystallinity is closely intertwined with their geological origin, and as e.g. Švarcová et al. (2011a) showed, the comparison with reference materials can lead to specification of the clay minerals' provenance. Hradil et al. (2011) used X-ray diffraction for differentiation of clay minerals present in green earths (clay micas like glauconite, celadonite, less commonly also chlorites or smectites). The results indicated that the Bohemian green earth from Kadaň has a relatively low celadonite content accompanied by interstratified celadonite/smectite, or smectite as a single phase. It gives rise to a forest

to olive green colour of the pigment compared to blue-green colouring of pure celadonites known from Italy or Cyprus, other popular deposits of green earth pigments.

Švarcová (2011) notes that mineralogical approach can be applied also on differentiation of natural and synthetic copper pigments like azurite and malachite. These copper carbonates are usually formed in oxidation zones of copper deposits; in such environment, they are accompanied by small amounts of various other minerals containing metal elements like As or Zn. The preparation and purification treatments of natural pigments do not remove these accompanying mineral phases. Furthermore, synthetic malachite grains are more uniform in size in contrast to natural malachite pigment. Therefore, thorough SEM-EDS analysis of the paint layer and evaluation of shape of the pigment grains can lead to successful differentiation of natural and artificially prepared copper carbonates' pigments.

Deeper understanding of mineralogy brings insight into numerous aspects of pigments' study. It enriches the knowledge about historic painting materials, their extraction, usage as well as degradation processes.

2.3 MINERAL PIGMENTS IN FINE ART – BRIEF OVERVIEW

Creation of art has been part of human nature since prehistoric times. Pigments have been obtained from natural sources, either in the form of minerals/rocks, or in the form of organic dyes gained from plants or various animals. The majority of minerals have naturally the colour appealing for pigment usage, and were only ground, washed and purified. Others were extracted and further treated, such as palygorskite, which served as a base for indigo in the preparation of a famous historical Central American pigment, Maya blue (Arnold et al., 2012). Some of the pigments have been prepared artificially; in Europe, the boom of synthetic pigments has been foreshadowed by the preparation of Prussian blue, a hydrated ferric hexacyanoferrate complex, in 1704 (Samain et al., 2013). Some of the inorganic synthetic pigments have natural mineral analogues, others are organic compounds which became popular in the 20th century European art due to their cheapness, availability and bright hues. However, their main drawback is their low chemical as well as colour stability.

The first mineral pigments documented e.g. in Palaeolithic cave paintings are earths (Iriarte et al., 2009; Beck et al., 2014; Olivares et al., 2013). The term 'earths' encompasses a wide range of natural materials; their mineral composition with different proportions of clay minerals, iron oxides/hydroxides, manganese oxides etc. determines their resulting colour. Thanks to their mineralogical variability, a relatively wide colour palette could be achieved including various hues of white, yellow, orange, red, brown or almost black. The cave paintings have also been created by iron red and yellow to brown ochres, which contain hematite or goethite, respectively, as the main component (Eastaugh et al., 2004).

In ancient Egypt, the variety of employed mineral pigments has been enriched by widely-employed white gypsum, calcite, huntite (trigonal $\text{CaMg}_3(\text{CO}_3)_4$) and yellow orpiment, a monoclinic arsenic sulphide (Eastaugh et al., 2004; Ambers, 2004). Orpiment has been identified e.g. in yellow parts of rich decorations in the tomb of Menna and in the tomb of Amenhotep III, both located in Luxor, Egypt (Vandenabeele et al., 2009; Uda, 2004). Another mineral yellow, but with more restricted usage, is described by Ambers (2004). He identified a trigonal sodium iron sulphate hydroxide, (natro)jarosite, in the yellow skin of a female figure and in two other Egyptian artefacts, which are currently in the British Museum and

were dated to ca 2600-2300 BC. Rarely, yellowish orange to red hues were created by crocoite, a monoclinic lead chromate, which has been detected in several funerary artefacts by Edwards et al. (2004). Rare findings are reported also in case of red mineral sulphides – realgar (monoclinic As_4S_4) and cinnabar (cubic HgS) (David et al., 2001; Bonizzoni et al., 2011). For creation of light blue hues, chrysocolla, a hydrated copper silicate, could be employed (Eastaugh et al., 2004). In this period of time, mineral pigments started to be prepared synthetically, especially those which were not readily available for extraction. These included e.g. the so-called Egyptian blue, mineralogically cuprorivaite (tetragonal $CaCuSi_4O_{10}$), an intensely blue pigment which has been identified in numerous works of Egyptian cultural heritage (Mahmoud, 2012; Bonizzoni et al., 2011; Pagès-Camagna et al., 2010).

The era of ancient Greece and Rome brought usage of azurite, a basic copper carbonate, which has been mentioned already by Theophrastus (ca 315 BC). It remained an important blue pigment up to the 17th century (Eastaugh et al., 2004). Green hues could be created using green earth, which is composed mainly of clay micas celadonite or glauconite, more rarely of other clay minerals. Famous deposits of high-quality celadonite-rich earths productive from Roman times to the 20th century are Monte Baldo, close to Verona, Italy, and Troodos Massif, Cyprus (Hradil et al., 2011). Clementi et al. (2011) have identified green earth rich in celadonite in the wall paintings of the Gilded Vault in Domus Aurea, an impressive imperial palace of Nero in ancient Rome. The artificially prepared minerals encompassed bluish green to green hoganite, a neutral variety of green copper acetates known as verdigris, which was prepared by corrosion of copper plates. Somewhat similar procedure, starting with acetic acid corrosion of lead plates, was used for the preparation of hydrocerussite. It became one of the most widespread white pigments and is known as lead white (Eastaugh et al., 2004).

Mediaeval times in Europe brought the usage of malachite, another basic copper carbonate, and have witnessed synthetic preparation of both azurite and malachite as well as widening of green and blue copper pigments' variety, including posnjakite, brochantite, pseudomalachite or atacamite. An expensive blue pigment imported from the area of today's Afghanistan, ultramarine, has been used predominantly in significant works of art and in iconographically important parts of paintings. It has been prepared from lapis lazuli by crushing, grinding and specialised purification which ensured high percentage of intensely blue lazurite grains in the resulting pigment (Eastaugh et al., 2004). Pérez-Arantegui et al. (2013) and Clark et al. (2010) report the usage of sky-blue aerinite, a complex monoclinic silicate, in Romanesque wall paintings in the region of Pyrenees, Spain. Subtle greyish blue hues have been created by vivianite, a monoclinic iron phosphate, e.g. in the 12th century wall paintings of the Winchester Cathedral, United Kingdom (Howard, 2003). Among the rare pigments belongs also purple to violet fluorite; its naturally irradiated variety is commonly called antozonite. It has been used mainly in the period between ca. 1450 and ca 1550 in Central European region, Germany, Switzerland and The Netherlands (Richter et al., 2001; Chlumská et al., 2010; Spring, 2007-8; Spring, 2000).

In the 18th century, hematite and goethite started to be produced synthetically, and were denominated Mars red and Mars yellow (in alchemy, Mars symbolised iron). At the end of the 18th century, the search for alternatives of widely used toxic lead white resulted in the employment of a synthetic white pigment called zinc white, mineralogically zincite (Eastaugh et al., 2004). Gradually, it became a very popular pigment, and was identified e.g. in the

works of Vincent Van Gogh (Salvant Plisson et al., 2014). Another modern mineral white pigment, which started to be used at the earlier 19th century, is synthetic baryte. It was employed as a pigment and extender, but it can be more commonly encountered as a part of lithopone, a co-precipitated pigment composed of barium sulphate and zinc sulfide (Eastaugh et al., 2004). Chrome yellow, mineralogically crocoite, started to be commercially produced in England between 1814 and 1816 (Eastaugh et al., 2004) and became a very popular pigment; later on, it has been complemented by another yellow pigment called cadmium yellow, most often hexagonal CdS analogous to greenockite. Cadmium yellow was detected e.g. in the work of Henri Matisse (*The Joy of Life*), one of the most influential painters of the 20th century (Mass et al., 2013). Finally, the 20th century brought commercial synthetic production of titanium dioxide white, both in the form of tetragonal rutile and tetragonal anatase. Bacci et al. (2007) document its usage in two oil paintings from the Gallery of Modern Art in Florence, while Franquelo et al. (2012) showed the usage of synthetic rutile and anatase in retouching on the example of a heavily retouched mediaeval polychrome sculpture.

2.4 PIGMENTS SELECTED FOR THIS STUDY

For this Ph.D. research, pigments were selected based on several criteria. The first one was the usability for provenance or authorship studies; another aspect was the tendency to degradation, and finally, undescribed analytical detection of the pigment in micro-samples.

Vivianite, a monoclinic hydrated ferrous phosphate, meets all the above-mentioned characteristics. It is a rare blue pigment, which has been identified in only about seventy works of European art. It seems to be used consistently by certain painters, as a sign of author's preference, therefore, can be used for authorship/provenance studies. Since it is formed in various geological settings, its elemental composition and morphology may indicate the regional provenance of the pigment. Furthermore, due to the content of divalent iron, it is prone to oxidative degradation. This process is accompanied by structural and colour changes observed in actual works of art, and it was suspected that external conditions may influence the processes. The occurring degradation complicates the analytical detection of vivianite or its degradation products in micro-samples of works of art and no procedure has been established for their reliable identification.

A not very-well described analytical detection in micro-samples along with potential usage for authorship/provenance studies is characteristic for a rare violet pigment fluorite, or its naturally irradiated form commonly called antozonite. Its Raman spectrum seems to be influenced by radiation-induced defects, thus producing a specific response to this analytical technique.

Copper-based pigments represent a wide group of minerals with similar elemental composition and different structure. They have been widely used; nevertheless, they can provide information essential for authorship/provenance ascription due to the presence of structural polymorphs or characteristic admixtures. Some of the copper pigments have tendency to degrade, which may result in the presence of other copper-based phases not originally present in the paint layer. An interesting degradative behaviour was observed in case of hoganite, neutral copper acetate, which loses its crystalline structure, thus presenting the micro-analysis with another problem to pursue. The theme of copper-based

pigments is very wide. In the present thesis, the focus is placed on aspects which have not been previously studied.

Both natural copper-based pigments and antozonite were extracted as a by-product of metal mining industry: copper ore and silver ore, respectively. As they have been obtained on important deposits, their characteristic mineral admixtures or trace elemental composition can indicate their provenance and thus help in the dating of the work of art (the deposits were usually mined over a restricted period of time). Another group of painting pigments related to metal ores extraction are Fe-based pigments, which together with a large group of clay-based pigments form an important and extensive part of the historical painting materials. However, these two groups are beyond the scope of this work.

Finally, pigments included in this study comprise also crocoite and orpiment (or its probable degradation product mimetite), which were identified in exceptional 13th century wall paintings in Kuřívody, Czech Republic.

3. EXPERIMENTAL

This chapter summarises studied mineralogical samples, which mainly served for testing of analytical methods and the study of specific mineral characteristics. It also gives a summary of artworks' micro-samples, which were first used for the definition of the studied problem, and then for testing of the results obtained on mineralogical samples and their usability in cultural heritage study and protection.

The chapter also describes the procedure of laboratory preparation of synthetic vivianite used for monitoring of its degradation processes, the creation of hoganite and vivianite model samples and subsequent experiments performed with vivianite. Finally, all the employed analytical methods and their specifications are described.

3.1 MINERALOGICAL SAMPLES

The mineralogical samples were obtained either from museums – National Museum in Prague, Czech Republic and Museum of Technische Universität Bergakademie Freiberg, Germany – or bought from reputable mineral and pigment dealers: Kremer Pigmente GmbH&Co. KG, Germany, and Minerály - Jiří Špalek, Czech Republic. One sample (yellow fluorite from Vrchoslav, Krupka) has been collected by the author.

Tab. 3-1 and 3-2 summarise the studied samples and their characteristics.

Tab. 3-1 Studied samples of naturally irradiated fluorite (antozonite), three differently coloured fluorites and synthetic fluorite standard

<i>Locality</i>	<i>Sample No.</i>	<i>Colour</i>
<i>Czech Republic</i>		
Jáchymov	1, 2	black
Vlastějovice	3, 4	violetish black
<i>Germany</i>		
Nabburg, Bavaria	5	violetish black
Nabburg, Bavaria	6, 7	black
Johanneschacht, Wölsendorf, Bavaria	8, 9	black
Johanneszeche, Wölsendorf, Bavaria	10, 11	black
Marienschacht, Wölsendorf, Bavaria	12, 13	black
<i>Mexico</i>		
Melchor Múzquiz, Múzquiz Municipality, Coahuila de Zaragoza	14	very deep violet
<i>Poland</i>		
Krzyżatka	15, 16	black
<i>China</i>		
Yaogangxian, Hunan Province,	17	bluish
<i>Czech Republic</i>		
Harrachov	18	green
Vrchoslav, Krupka	19	yellow
<i>synthetic fluorite from Sigma Aldrich</i>	S. A.	white

Tab. 3-2 Studied samples of vivianite

<i>Locality</i>	<i>Sample No.</i>	<i>Inventory No. of the original sample, source^a</i>	<i>Morphology of vivianite in the original sample</i>	<i>Available information</i>
<i>Australia</i>				
Wannon River	viv 5	P1N 18760, NM	crystal druse	in clay underlying basalt rock (Pratesi et al., 2003)
<i>Bolivia</i>				
Tomokoni, Canutillos, Colavi, Potosí	viv 10	Minerály - Jiří Špalek	single crystal on Fe-rich matrix	information not available; limonite (?)
<i>Cameroon</i>				
Anloua	viv 3	non-inventoried, TUBF	fan-shaped radiating crystals	lacustrine sedimentary basin (http://www.mindat.org/loc-55149.html)
<i>Colombia</i>				
?	viv 2	Kremer Pigmente GmbH&Co. KG	pulverised crystals	commercially available pigment; no Colombian locality of vivianite is stated in the mineralogical literature
<i>Czech Republic</i>				
Litošice	viv 7	P1N 18735, NM	crystals	in oxidation zone of Mn and Fe ore deposit (graphitic shales with pyrite overlaid by Mn carbonates) (Kratochvíl, 1961)
Mariánské Lázně	viv 19	P1N 18743, NM	bulbous aggregates and voids' fillings	peat bog (information on the label accompanying the sample)
Františkovy Lázně	viv 20	P1N 18742, NM	bulbous aggregate	peat bog (information on the label accompanying the sample)
<i>Germany</i>				
Amberg	viv 9	non-inventoried, TUBF	crystals	limonite (Bernard and Rost, 1992)
Eckartsberga	viv 8	non-inventoried, TUBF	powder	limestone (Klaproth, 1807)
Hagendorf	viv 16	non-inventoried, TUBF	earthy aggregate	Mn-rich pegmatite (Dill, 2009)
Rönneburg	viv 12	57424, TUBF	earthy aggregate	information not available; limestone (?)
<i>Ukraine/Russia</i>				
Kerch	viv 4	Minerály - Jiří Špalek	crystal in fossilised shell	iron ore basin (Bernard and Rost, 1992)

^a NM = National Museum (in Prague, Czech Republic)

TUBF = Technische Universität Bergakademie Freiberg (Germany)

3.2 ARTWORKS' MICRO-SAMPLES

Preparation of the micro-samples: RNDr. J. Hradilová, Mgr. P. Bauerová, Mgr. V. Vašutová

The micro-samples of works of art were obtained usually from restorers during restoration/conservation campaigns.

The obtained micro-samples were either left as loose fragments (usually for the analysis by micro-X-ray diffraction or vibrational spectroscopies), or embedded in polyester resin Neukadur PE 45, ground and studied in cross-section.

Tab. 3-3 summarises the studied micro-samples; they are categorized according to the minerals which were the main subject of this study.

Tab. 3-3 List of analysed micro-samples – Part I: vivianite

<i>Code</i>	<i>Author, artwork, place</i>	<i>Type of artwork</i>	<i>Dating of the original painting</i>
D4	Anonymous Master, Passion Altar from Dupuș, church in Mediaș, Romania	Easel painting	80s of the 15 th C
J1006-1	Jean George de Hamilton, Portrait of a horse Flery with groom, Hluboká Castle, Czech Republic	Easel painting	—
J1008-1	Jean George de Hamilton, Portrait of a horse called Buffon (black groom), Hluboká Castle, Czech Republic	Easel painting	—
J1009-1	Jean George de Hamilton, Portrait of a horse with turkish groom, Hluboká Castle, Czech Republic	Easel painting	1713
J1211-1	Jean George de Hamilton, Portrait of a bay horse with groom, Hluboká Castle, Czech Republic	Easel painting	1704
J1212-2	Jean George de Hamilton, Portrait of a white horse with groom, Hluboká Castle, Czech Republic	Easel painting	1705
J1213-1	Jean George de Hamilton, Portrait of a white horse with black groom, Hluboká Castle, Czech Republic	Easel painting	1705
J1214-3	Jean George de Hamilton, Portrait of a bay horse Mignon, Hluboká Castle, Czech Republic	Easel painting	1705

Tab. 3-3 List of analysed micro-samples – Part II: naturally irradiated fluorite (antozonite)

<i>Code</i>	<i>Author, artwork, place</i>	<i>Type of artwork</i>	<i>Dating of the original painting</i>
J1325-1hv	Anonymous Master, Triptych with St. Jacob the Younger and St. Philip, chapel of St. Wenceslaus and St. Ladislaus, Italian Court, Kutná Hora, Czech Republic	Easel painting	1497
J1325-U	Anonymous Master, Triptych with St. Jacob the Younger and St. Philip, chapel of St. Wenceslaus and St. Ladislaus, Italian Court, Kutná Hora, Czech Republic	Easel painting	1497

Tab. 3-3 List of analysed micro-samples – Part III: crocoite and mimetite

<i>Code</i>	<i>Author, artwork, place</i>	<i>Type of artwork</i>	<i>Dating of the original painting</i>
J1223-3	Anonymous Master, St. Dorothy – rose, St. Gallus church, Kuřívody, Czech Republic	Wall painting	before 1300
J1223-4	Anonymous Master, Virgin Mary – kerchief, St. Gallus church, Kuřívody, Czech Republic	Wall painting	before 1300
J1223-14	Anonymous Master, St. Dorothy – clothing, St. Gallus church, Kuřívody, Czech Republic	Wall painting	before 1300
J1223-15	Anonymous Master, St. Dorothy – rose, St. Gallus church, Kuřívody, Czech Republic	Wall painting	before 1300
J1223-16	Anonymous Master, St. Dorothy – clothing, St. Gallus church, Kuřívody, Czech Republic	Wall painting	before 1300

Tab. 3-3 List of analysed micro-samples – Part IV: copper pigments

<i>Code</i>	<i>Author, artwork, place</i>	<i>Type of artwork</i>	<i>Dating of the original painting</i>
10-376-I-5	Hans-Jakob Sprüngli, Venus and Cupido, Museum of Decorative Arts, Prague, Czech Republic	Reverse painting on glass	around 1610
J0517-3	Anonymous, Madonna with Child Jesus, St. Laurence church, Černá Hora, Czech Republic	Polychromy on wood	around 1500
J0634-1	Workshop of the Master of the Matejovce Altarpiece, The Gothic triptych of St. King Steven and St. Imrich, St. Stephan King church, Poprad - Matejovce, Slovakia	Panel painting	after 1453
J0914-5	Unknown master (H.E.R), Prayer at Mount of Olives, Church of St. Bishop Martin of Tours, Lipany, Slovakia	Panel painting	1526
J1120-1	Anonymous, Madonna – Sedes Sapientiae, private owner, Czech Republic	Polychromy on wood	12 th C
Lacko-2	Anonymous, Announcing Archangel (wing of the triptych), Lacko, Poland	Panel painting	2 nd quarter of the 15 th C
M0118-3	Francesco Novellino, Altar (wood carving), Prague Municipal Museum, Czech Republic	Wax relief on wood	1 st quarter of the 17 th C
M0356-6	Micheil van Coxie, St. John the Evangelist, double-faced altar wings, National Gallery in Prague, Czech Republic	Panel painting	around the half of the 16 th C
M0366-8	Anonymous, Decapitation of St. Catherine, Wallachian Open Air Museum, Rožnov pod Radhoštěm, Czech Republic	Easel painting Oil on canvas	17 th C?
M0412-1	Anonymous, Virgin Mary with Child Jesus and St. Anna, private owner, Czech Republic	Easel painting Oil on canvas	18 th C
M0415-2	Anonymous, Crucifixion, Roman-Catholic Church of St. John Baptist, Hlučín, Czech Republic	Panel painting	1540-1560
M0424-1	Anonymous, St. Joachim, Church of the Annunciation, Vlachovo Březí, Czech Republic	Polychromy on wood	18 th C
M0426-5	Anonymous, Altarpiece Epitaph of Benedict Umlauf – part The Holy Trinity, Cathedral of St. Peter and Paul, Brno, Czech Republic	Panel painting	1612
M0604-2A	Anonymous, Angel, private owner, Czech Republic	Polychromy on wood	18 th C ?
M0608-4	Unknown Czech Master, Assumpta from White Mountain, National Gallery in Prague, Czech Republic	Easel painting	around 1450
M0610-4	Anonymous, Lunette depicting the scenes from the life of St. Francis (1), Minorite Monastery in Český Krumlov, Czech Republic	Easel painting	1658
M0713-3	Master of Chudevický Altarpiece - Šimon Láb?, Votive panel of Švihovský Family, Roman-Catholic church of St. Michael, Horažďovice, deposited in National Museum in Prague, Czech Republic	Panel painting	1504-1505
M0744-2	Anonymous, Lunette depicting the scenes from the life of St. Francis (2), Minorite Monastery in Český Krumlov, Czech Republic	Easel painting Oil on canvas	17 th C
M0819-4	Anonymous, Sculpture of saint, Civil association, Pernštejn, Czech Republic	Polychromy on wood	18 th C
M0821-1	Anonymous, St. John the Baptist, Civil association, Pernštejn Czech Republic	Polychromy on wood	18 th C
M0914-2	Anonymous, Kosma and Damian, Congregation of the Sisters of Mercy of St. Charles Borromeo – Prague, Czech Republic	Polychromy on wood	17/18 th C

3.3 MODEL SAMPLES

3.3.1 HOGANITE MODEL SAMPLES

Model Mixtures with Lead Pigments

Sample preparation: Ing. Silvie Švarcová, Ph.D.

Model mixtures of hoganite with lead white and lead tin yellow were prepared in order to determine the detection limit of hoganite in highly absorbing matrix by the means of powder XRD and to evaluate possible negative effect of such matrix on the identification of verdigris in paint layers. Two-phase mixtures with 0.5, 1, 2, 5, 10 and 20 wt. % hoganite with the corresponding amount of PbCO₃ and/or Pb₂SnO₄ were prepared by thorough grinding of both pigments in an agate mortar. Resulting sets of model mixtures were analysed by powder XRD.

Model Paint Layer Samples

Sample preparation: Ing. Silvie Švarcová, Ph.D.

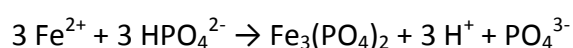
Interactions of hoganite with proteinaceous binders were studied on a set of model samples. Skin glue, egg yolk and whole egg binders were prepared according to the painting procedure; subsequently, they were used for the creation of temperas with various content of hoganite. Its content (5 and 10 %) was given in weight percentage related to the global content of the binder and the hoganite.

To monitor both the influence of binders and of the highly diffracting phases, another set of model paint layer samples with lead tin yellow I (Pb₂SnO₄) were created. The amount of the Pb₂SnO₄ was equal to the amount of hoganite, i.e. 5 and 10 wt. % hoganite, 5 and 10 wt. % Pb₂SnO₄ in 90 and 80 wt. % skin glue or egg, respectively. Skin glue was used in the form of freshly prepared 5 wt. % aqueous solution. For the egg yolk tempera, egg yolk was separated from the white and the egg yolk membrane was carefully removed. The obtained yolk was mixed with distilled water in the 1:1 weight ratio. To prepare the whole egg tempera, the egg yolk was separated. Then, the egg white was whipped and, subsequently, the foam was left to settle down for about one hour. The fluid was decanted and mixed with egg yolk. Typically, the weight ratio of egg yolk to treated egg white was 1:2.5. Pigments were thoroughly mixed and ground with the binders to create the resulting temperas. Those were applied on glass or non-diffraction Si support using brush.

3.3.2 SYNTHESIS OF VIVIANITE

Synthesis design: Ing. S. Švarcová, Ph.D.; synthesis: Ing. S. Švarcová, Ph.D., RNDr. Z. Čermáková, G.G.

In order to prepare model samples with undegraded vivianite, the mineral has been prepared synthetically, by a precipitation reaction. Since the reported procedures (Mattievich and Danon, 1977) led to multicomponent products (e.g. the recommended method of Evans resulted in a mixture of vivianite and spheniscidite, (Fe₂(NH₄)(OH)(PO₄)₂·2H₂O), the method has been adapted. The precipitation reaction was carried out according to a general principle:



An appropriate amount of $\text{FeSO}_4 \cdot 7\text{H}_2\text{O}$ p.a. (Lachema Neratovice) was dissolved in 5 wt. % solution of H_3PO_4 (Merck) with a final molar concentration of Fe being 0.28 mol/l. A stoichiometric quantity of $\text{Na}_2\text{HPO}_4 \cdot 12\text{H}_2\text{O}$ p.a. (Lachema Neratovice) was dissolved in distilled water and added drop by drop by peristaltic pump (ca 3 ml/min) into the solution of FeSO_4 and H_3PO_4 under continuous magnetic stirring. The resulting mixture was then stirred until the following day under laboratory conditions. Subsequently, the bluish grey precipitate was left to settle for 24 hours. The resulting product was separated by centrifugation and washed by distilled water. The centrifugation showed that the resulting product is formed by whitish and blue precipitates with different density, therefore, they were separated by the centrifugation process. The final blue precipitate was left to dry on air under laboratory conditions and checked by X-ray diffraction as well as Mössbauer spectroscopy, which showed that it is phase pure vivianite with 15% of Fe^{3+} . The whitish by-product was found to be amorphous phosphate with 94% of Fe^{3+} .

3.3.3 VIVIANITE MODEL SAMPLES

Model Paint Layer Sample I

Sample preparation: Mgr. P. Bauerová, RNDr. Z. Čermáková, G.G.

To better understand the morphology of vivianite grains of different geological origin in the paint layer (vivianite pigment grains of the naturally powdery samples vs. those created by grinding crystals) and to compare it with the grain morphology present in the micro-samples of works of art, a model sample composed of lead white + chalk (calcite) ground and lead white + vivianite pigment composed of ground up crystals (Kremer Pigmente) has been prepared. Then, a micro-sample was obtained, embedded in a polyester resin Neukadur PE 45, ground and studied in cross-section.

Model Paint Layer Samples II

Sample preparation: RNDr. Z. Čermáková, G.G.

For the evaluation of the behaviour of vivianite under increased-temperature conditions and of the potential effect of the present binder, the prepared synthetic vivianite was mixed with four main historic binders, i.e. oil (linseed stand oil Kremer Pigmente), egg yolk (egg from bio-farming, egg yolk separated from egg white and pierced through gauze to ensure that no egg membrane enters the paint), glue (5% solution of rabbit glue Graz in distilled water, gently heated to 60°C) and water (distilled). To study potential differences between the synthetic and powdered natural samples, natural crystals from Bolivia (equivalent to viv 10, Tab. 3-2) were first cleaned of the iron-rich matrix, ground and mixed with distilled water.

Vivianite with each separate binder was ground in an agate mortar so the pigment would sufficiently bind with the binder and thus create a resulting paint of good quality. The binders were added in such amount that a paint of satisfactory density was prepared (which has been consulted with restorer). Two samples of each type of paint (one for the experiment and one as a reference) were created and applied on glass slides. After that, the samples were kept in dark. Vivianite with oil was prepared as the first type of model samples and was left to dry for 7 months. Other mixtures were dry in less than a week.

Oil-on-canvas Mock-ups

Sample preparation: MgA. T. Tichý, RNDr. Z. Čermáková, G.G.

To test the effect of increased temperatures on vivianite paint, which may take place in praxis (i.e. relining of canvas paintings relining, which basically consists of ironing a new canvas on the back of the old degraded one using various organic compounds), two small canvases were created (one for relining, one as a reference). The employed painting technique was inspired by the one used e.g. by Jean George de Hamilton, a painter of the end of the 16th and the beginning of the 17th century active (among others) in the region of today's Czech Republic.

First, a ground was prepared using iron-rich earths (Red Bole, Kremer Pigmente + glue solution + linseed stand oil Kremer Pigmente + beeswax). Then, on both canvases, three squares of oil paint were applied, freshly ground-up natural vivianite crystals (described above) with:

- 1) oil (linseed stand oil UMTON) and a few drops of turpentine (balsam turpentine Kremer Pigmente),
- 2) oil, a few drops of turpentine and lead white (Kremer Pigmente, Kremser White 46 000) (vivianite:Pb white approx. 40:60),
- 3) oil, a few drops of turpentine and lead white (vivianite:Pb white approx. 10:90).

After relining, micro-samples were obtained from both the relined and the reference oil-on-canvas mock-ups. They were embedded in polyester resin Neukadur PE 45, ground and polished in cross-section.

3.4 MODEL EXPERIMENTS WITH VIVIANITE

3.4.1 HIGH TEMPERATURE X-RAY DIFFRACTION EXPERIMENT (IN SITU)

Institute of Inorganic Chemistry of the ASCR, v.v.i., Dr. RNDr. P. Bezdička

High temperature diffraction patterns were collected on PANalytical X'Pert PRO diffractometer equipped with conventional X-ray tube (Co K α radiation, 40 kV, 30 mA, line focus) and a multichannel detector X'Celerator with an anti-scatter shield together with high temperature chamber (HTK 16, Anton Paar, Graz, Austria). X-ray patterns were measured at 25°C and between 40°C and 200°C with a step of 10°C in the range of 10 to 50° 2Theta (step of 0.0334° and 100 s counting per step yielding a scan of ca 16 minutes) using conventional Bragg-Brentano geometry. The measurements were performed while the sample was heated to the designated temperature, i.e. in situ.

3.4.2 TEMPERATURE EXPERIMENTS (EX SITU)

Institute of Inorganic Chemistry of the ASCR, v.v.i., RNDr. Z. Čermáková, G.G.

The model paint layer samples (both the ones to be heated and the reference ones) were, before the heating experiments started, measured by UV-VIS spectrophotometry, Fourier-transform infrared spectrometry (FT-IR), XRD and analysed by optical microscopy. Then, one set of the model paint layer samples was inserted into the oven and heated in separate steps to 60°C, 80°C, 100°C, 120°C, 160°C and 200°C. After every heating step, the samples were measured by UV-VIS spectrophotometry and photographed. After every

second step (80°C, 120°C, 200°C), all the following analyses were performed on all the heated samples: UV-VIS, FT-IR, XRD and optical microscopy. The measurements were performed after the samples were exposed to heating, i.e. ex situ.

For the heating, a Memmert oven was used enabling a very precise programming of the heating process. The samples were inserted into the oven and the desired temperature was input. The heating until the desired temperature was set to full power; after the input temperature was achieved, it was held for 30 minutes. Then, the fan was programmed to 100% while the heating was turned off and the cooling took place during 10 minutes. After that, the samples were removed from the oven and let cool down to room temperature.

3.4.3 CONSERVATION TECHNIQUE – RELINING

Academy of Fine Arts in Prague, MgA. T. Tichý, RNDr. Z. Čermáková, G.G., Mgr. V. Vašutová

For the execution of the traditional relining, bleached beeswax and damar resin (both from art materials supplier Zlatá Loď, Prague, Czech Republic) were used. 50 ml of damar resin was mixed with 100 ml of beeswax and 30 ml of turpentine (Kremer Pigmente fir turpentin) and heated. For the monitoring of temperature to which the vivianite-containing paint is exposed during the procedure, two types of irreversible temperature indicators (Testoterm, Testo AG, Lenzkirch) were employed, one type covering the temperature range from 37 to 65°C, the other from 71 to 110°C, both with steps of 3 to 6°C. These were applied before the relining to the painted side of the canvas. During the relining, the temperature was also monitored by an infrared thermometer Voltcraft IR-364 (optics: 30:1).

The relining was performed in a traditional way using iron (Westby, 1974; Boissonnas and Diethelm, 1981).

3.4.4 HUMIDITY EXPERIMENTS

Academy of Fine Arts in Prague, RNDr. Z. Čermáková, G.G., Mgr. V. Vašutová

To evaluate the influence of increased humidity on vivianite, two types of vivianite model paint layer samples II (ground natural vivianite prepared with water and synthetic vivianite with water) were inserted into CLIMACELL 111 climate chamber (BMT Medical Technology) and left there for three weeks under room temperature (25°C) and 90% relative humidity.

3.5 ANALYTICAL METHODS

3.5.1 OPTICAL MICROSCOPY, PHOTOGRAPHY

Academy of Fine Arts in Prague and Institute of Inorganic Chemistry of the ASCR, v.v.i., RNDr. J. Hradilová, Mgr. V. Vašutová, RNDr. Z. Čermáková, G.G.

Optical microscopy has been used for the study of micro-samples, both in visible (VIS) and UV light. Two microscopes were used: Olympus BX 60 (VIS, UVA 330-380 nm) equipped with Olympus digital camera DP70 and Axio Imager A.2 from Zeiss (VIS, 365 and 470 nm) with Olympus DP 75 digital camera.

Optical studies of vivianite model paint layer samples II heated to different temperatures were undertaken using Olympus BX 40 microscope equipped with DP 10 camera.

The macro-photographs of model paint layer samples II and oil-on-canvas mock-ups were taken together with a standard grey plate, which was later on used to refine the colours in Adobe Photoshop Lightroom, therefore, their colouring is accurate and comparable to each other.

3.5.2 PORTABLE X-RAY FLUORESCENCE

Academy of Fine Arts in Prague, RNDr. J. Hradilová, Mgr. D. Hradil, Ph.D.

The non-invasive X-ray fluorescence (XRF) measurements of the wall paintings in Kuřívody, Czech Republic, were carried out in situ using two hand-held energy dispersive XRF spectrometers: XMET 3000 TXR by Oxford Instruments, UK (Rh anode, voltage 40 kV, Si-PIN detector) and Delta Premium by Innov-X, USA (Rh anode, voltage 40 kV, silicon drift detector (SDD)). This method has provided information about the distribution of chemical elements heavier than calcium ($Z > 20$, X-MET) or magnesium ($Z > 12$, Delta), respectively. The measurements were performed in air; therefore, the identification of lighter elements was prevented.

3.5.3 SCANNING ELECTRON MICROSCOPY – ENERGY DISPERSIVE SPECTROSCOPY

Institute of Inorganic Chemistry of the ASCR, v.v.i., RNDr. Z. Čermáková, G.G., Ing. S. Švarcová, Ph.D.

The micro-samples of works of art containing copper pigments were studied mainly by the Philips XL30 CP scanning electron microscope equipped with Robinson detector of back-scattered electrons working under constant pressure of 50 Pa and an accelerating voltage of 25 kV. Elemental microanalyses were carried out using EDAX energy-dispersive spectrometer equipped with compact sapphire Si(Li) detector and light elements performance technology (LEAP+) allowing the detection of elements heavier than Be ($Z > 4$) at resolution of 135 eV. Later on, micro-samples as well as mineralogical and model samples were studied by Jeol JSM6510 scanning electron microscope equipped with energy-dispersive spectrometer INCA (Oxford Instruments) with SDD detector allowing detection of elements heavier than Be ($Z > 4$) at 125 eV resolution. Measurements were carried out in a low vacuum mode under the pressure of 30 Pa and accelerating voltage of 25 kV; backscattered electrons were detected. In both cases, low vacuum mode allowed analysis of samples without conductive coating of their surface.

3.5.4 X-RAY DIFFRACTION AND X-RAY MICRO-DIFFRACTION

Institute of Inorganic Chemistry of the ASCR, v.v.i., Dr. RNDr. P. Bezdička, RNDr. Z. Čermáková, G.G., Ing. S. Švarcová, Ph.D.

Diffraction patterns of vivianite mineralogical samples and of vivianite model paint layer samples II were collected on PANalytical X'Pert PRO diffractometer equipped with conventional X-ray tube ($\text{Co}_{K\alpha}$ radiation, 40 kV, 30 mA, line focus) and a multichannel detector X'Celerator with an anti-scatter shield. X-ray patterns were measured in the range of 6 to 110° 2θ with the step of 0.0167° and 120 s counting per step (total time of the scan: approx. 1.75 hours), using conventional Bragg-Brentano geometry.

Diffraction patterns of naturally irradiated fluorites were collected using a PANalytical X'Pert PRO diffractometer equipped with a conventional X-ray tube ($\text{Cu}_{K\alpha}$ 40 kV, 30 mA, line focus) in transmission mode. An elliptic focusing mirror, a divergence slit 0.5° , an anti-scatter slit 0.5° and a Soller slit of 0.02 rad were used in the primary beam. A fast linear position sensitive detector PIXcel with an anti-scatter shield and a Soller slit of 0.02 rad were used in the diffracted beam. All patterns were collected in the range of 22 to 88° 2θ with the step of 0.013° and 900 sec/step resulting in a scan of about 5 hours. Unit cell refinement has been performed by the least squares method, as implemented in the HighScorePlus software and AFPAAR programme.

The micro-diffraction of all the studied micro-samples either in the form of fragments of colour layers or as their cross-sections embedded in polyester resin was performed also on PANalytical X'Pert PRO, this time with $\text{Co } K\alpha$ tube with point focus, an X-ray monochromator with a diameter of 0.1 mm, and a multichannel detector X'Celerator with an anti-scatter shield. X-ray patterns were measured in the range of 4 to 80° 2θ with the step of 0.034° and 2200 s counting per step (total time of the scan: approx. 11.2 hours).

XRD patterns were not pre-treated before interpretation as no background correction was needed. Qualitative analysis was performed using HighScorePlus software package (PANalytical, The Netherlands, version 3.0.5), Diffrac-Plus software package (Bruker AXS, Germany, version 8.0) and JCPDS PDF-2 database (2004).

3.5.5 RAMAN SPECTROSCOPY

Institute of Geochemistry, Mineralogy and Mineral Resources, Faculty of Science, Charles University in Prague, prof. J. Jehlička, Mgr. K. Osterrothová, Ph.D., Mgr. A. Culka, Ph.D., RNDr. Z. Čermáková, G.G. Department of Inorganic Chemistry, Faculty of Science, Charles University in Prague, RNDr. Z. Čermáková, G.G., doc. RNDr. I. Němec, Ph.D., Mgr. V. Košářová

Raman analyses of vivianite mineralogical samples as well as vivianite-containing micro-samples were performed on a multichannel Renishaw In Via Reflex microspectrometer equipped with a Peltier-cooled charge-coupled device detector using 785 nm and 514.5 nm excitation lasers. 50x objective was used for all the measurements. While using 785 nm laser, 1200 l/mm grating was employed; the powdery mineralogical samples were analysed using laser power of 3 mW, 20 s exposure time, 20 accumulations, the range being 1800 - 100 cm^{-1} . The range 3800 - 2600 cm^{-1} was attempted, but no signal has been achieved. Mineralogical samples in the form of crystals could be analysed using 30 mW without alteration of the sample. Cross-sections of the micro-samples of the artworks were analysed by 1.5 mW, 10 s exposure time, 1 accumulation in the range of 1800 - 100 cm^{-1} . While using 514.5 nm laser, 1800 l/mm grating was used and the range was 1800 - 100 cm^{-1} and 3800 - 2600 cm^{-1} . Powdery mineralogical samples were analysed by 0.245 mW laser power, 10 s exposure time and 10 accumulations, the crystals were measured by 2.45 mW laser power having the same exposure time and number of accumulations. The cross-sections of the micro-samples were analysed using 0.245 mW, 10 s exposure time and 1 accumulation. The same conditions were set for the analysis of micro-samples in the form of loose fragments obtained from the works of art. The spectral resolution was 2 cm^{-1} . Raman spectra were exported into the Galactic *.SPC format; they were normally not subjected to any data manipulation or processing techniques.

Raman analyses of naturally irradiated mineralogical samples of fluorite and micro-samples containing fluorite, copper pigments, crocoite and mimetite were performed on a Thermo Scientific DXR Raman Microscope with Peltier-cooled CCD detector interfaced to an Olympus microscope (10x and 50x objective lens) in the 50–3400 cm^{-1} spectral region with 4 cm^{-1} resolution. The spectrometer was calibrated by software-controlled calibration procedure using multiple neon emission lines (wavelength calibration), multiple polystyrene Raman bands (laser wavenumber calibration) and standardised white light sources (intensity calibration).

The spectra of micro-samples were collected using 532 nm laser with 0.1 to 0.2 mW laser power, 32 scans and 2 s exposure time, 50x objective lens. For the analysis of mineralogical samples, four lasers of different wavelengths were used: 445, 532, 633 and 780 nm. Typical analytical conditions were following: 10x objective lens, 64 scans, 2 s exposure time, 10 mW laser power.

Two of the naturally irradiated fluorites (fluorite 3 and 13) were measured also by FT Raman spectrometer Thermo Nicolet 6700 FT-IR equipped with a Nexus FT Raman module (1064 nm Nd:YVO₄ laser excitation, Happ-Genzel apodization, 4 cm^{-1} resolution, 3700–150 cm^{-1} range), however, the samples exhibited strong fluorescence.

3.5.6 FOURIER-TRANSFORM INFRARED SPECTROSCOPY

Transmission

Institute of Inorganic Chemistry of the ASCR, v.v.i., J. Večerníková, RNDr. Z. Čermáková, G.G. (data interpretation)

The FT-IR measurements in transmission mode were performed using Thermo Scientific Nicolet NEXUS 670 FT-IR. The samples were analysed in KBr pellets. The amount of the sample for the analysis was ranging from 1.4 to 1.5 mg/300 mg KBr. The acquisition of the spectra comprised 64 scans in the range of 4000 – 400 cm^{-1} , resolution being 4 cm^{-1} .

Reflection

Polymer Institute Brno, Ing. Z. Vrátníčková, RNDr. Z. Čermáková, G.G. (data interpretation)
Faculty of Restoration, University of Pardubice, Mgr. E. Dytrychová, RNDr. Z. Čermáková, G.G. (data interpretation)

For the collection of micro-FT-IR spectra in the reflection mode of micro-samples either in the form of cross-sections or loose fragments, microscope Continuum and spectrometer Nexus were used, both produced by Thermo Scientific Nicolet. The data were collected using 512 scans, in the 4000 – 650 cm^{-1} range with the resolution of 8 cm^{-1} . Some of the spectra were obtained also on Thermo Scientific Nicolet iN10 microscope (256 scans, 8 cm^{-1} resolution with 4000-675 cm^{-1} range). The analysed area varied between 30x30 μm and 100x40 μm .

Micro-Attenuated Total Reflectance

Faculty of Restoration, University of Pardubice, Mgr. E. Dytrychová, Mgr. J. Havlín, RNDr. Z. Čermáková, G.G. (data interpretation)

Micro-FT-IR spectra in the micro-attenuated total reflectance mode (micro-ATR) were collected on Thermo Scientific Nicolet iN10 microscope equipped with germanium Slide-On

Micro-Tip ATR crystal (350 μm in diameter). Liquid nitrogen-cooled MCT detector enabled the measurement of particles or cross sections smaller than 10 μm (<https://static.thermoscientific.com/images/D12899~.pdf>, accessed 4 June 2013). The best results were obtained using 256 scans and 8 cm^{-1} resolution, the range being 4000-675 cm^{-1} . The applied pressure was very low (2 on the scale from 1 to 100). The nature of the measurement enabled the analysis of the samples only in the form of cross-sections embedded in the resin; the ATR crystal ensuring the optical contact with the sample would crush the fragile loose fragments of the paint layers. The analysed area varied between 20x20 μm and 100x40 μm .

3.5.7 MÖSSBAUER SPECTROSCOPY

Institute of Inorganic Chemistry of the ASCR, v.v.i., Ing. A. Lančok, Ph.D.

Mössbauer spectroscopy was employed for the determination of the ratio of Fe^{2+} and Fe^{3+} in the ground vivianite crystals from Bolivia, which were used for the creation of model paint layer samples II with water, oil-on-canvas mock-ups and studied by high-temperature X-ray diffraction.

The Mössbauer spectra measurement was carried out in transmission mode with ^{57}Co diffused into an Rh matrix as a source moving with constant acceleration at room temperature. The spectrometer (Wissel) was calibrated using a standard $\alpha\text{-Fe}$ foil, and the isomer shift was expressed with respect to this standard at 293 K. The fitting of the spectra was performed in CONFIT program (Žák and Jirásková, 2006). This program utilises a convolution algorithm in the fitting of the overlapped Mössbauer spectra. The program also integrates the fitting of the ratio of Fe^{2+} and Fe^{3+} atoms. It is able to work with 1024 experimental points per spectrum; the number of fitted parameters must not exceed 105 and the number of spectrum components must be less than or equal to 99.

To monitor the oxidation changes with increasing temperature, vivianite sample was heated in separate steps to 60°C, 80°C, 90°C, 100°C, 110°C, 120°C and 130°C. Each heating step took 30 minutes; after the sample cooled down to room temperature, Mössbauer analysis has been performed.

3.5.8 UV-VIS SPECTROPHOTOMETRY AND ANALYSIS OF IMAGE HISTOGRAMS

*Institute of Inorganic Chemistry of the ASCR, v.v.i., RNDr. Z. Čermáková, G.G., Ing. K. Lang, CSc.
Department of Inorganic Chemistry, Faculty of Science, Charles University in Prague, Mgr. Petr Henke
Institute of Information Theory and Automation of the AS CR, v.v.i., Mgr. J. Blažek*

The model paint layer samples II (vivianite with different historic binders) were measured by UV-VIS spectrophotometer Lambda 35 from Perkin Elmer Instruments using an integrating sphere. The samples of synthetic vivianite with oil (whose layer was very thin) were, during measurement, underlaid by a black pad to ensure that no incoming radiation pass through the sample and the glass. The obtained reflectance results were transformed into CIE L^*a^*b 1964 space using the Color program. The measurements were repeated after each heating step of the temperature experiments.

Two naturally irradiated fluorite samples (14 and 16 – as representatives of light and dark coloured samples) were measured by UV-VIS spectrophotometer Cary 4000 UV-VIS (Agilent) equipped with an integrating sphere. The measurement has been performed in diffuse reflectance mode to minimise light scattering. Since the dark coloured sample

exhibited complete absorption and it was not desirable to dilute the samples in order to prevent the contamination for following analyses, the evaluation of the samples' lightness has been performed by the analysis of image histograms. Each ground naturally irradiated antozonite sample was applied in a continuous flat layer on glass slide and photographed by Canon D500 Rebel camera under controlled light (D65 light source). Position of the sample, camera and light source were fixed and the camera parameters (shutter speed, aperture, objective, focus, white balance) were kept the same. These constant conditions ensured that the histograms of the photographs were comparable.

For the evaluation of the colour change of oil-on-canvas mock-up after relining which is too large to fit into the above-stated UV-VIS spectrophotometers, photographs of the vivianite paints were obtained using Canon D500 Rebel camera under similar conditions with fixed parameters as described above. These constant conditions ensure that the RGB coordinates of the photographs' pixels are comparable. The size of the taken photos was 417x433 for the reference mock-up and 427x446 for the relined one. This number of pixels results in more than 180 000 point measurements of RGB coordinates.

4. RESULTS AND DISCUSSION

This section summarises results presented in five papers accompanying this thesis in Appendix A. The first part focuses on crucial theme of micro-analysis of paint layers of works of art and how the correct identification of rare pigments like vivianite, fluorite and crocoite can provide essential information for provenance/authorship studies or dating. The micro-analysis of a large group of copper pigments is challenging due to their chemical similarity. They have been widely used, nevertheless, their specific characteristics may contribute to provenance determination, and their precise description is necessary for the complex evaluation of the work of art. The copper-based pigments will be covered in the final section of the first, micro-analytical part. In the second part focusing on pigment degradation, changes caused by internal agents (taking place in the complex environment of the paint layer) and those caused by external agents (conditions including increased temperature or humidity) will be presented with special attention to hoganite (neutral verdigris) and vivianite.

4.1 MICRO-ANALYSIS OF MINERAL PIGMENTS AND THEIR PROVENANCE/AUTHORSHIP STUDIES

For the micro-analysis of painting pigments, it is essential to know as much as possible about the studied materials. In case of mineral pigments, the study of mineralogical samples can provide information about their possible analytical response in micro-scale. Nevertheless, the limitations of micro-analytical methods and of the highly heterogeneous micro-samples make the correct and unambiguous pigment identification a challenge.

4.1.1 VIVIANITE

Vivianite is a phosphate mineral ($\text{Fe}_3(\text{PO}_4)_2 \cdot 8\text{H}_2\text{O}$) with monoclinic crystal structure. In nature, it can be found in the form of crystals or various types of aggregates; the prevailing aggregate type is the earthy one (Bernard and Rost, 1992). Earthy vivianite is a common mineral admixture in sedimentary reduction environments, including peat bogs, iron bog ores or lacustrine and marine sediments (Bernard and Rost, 1992; Fagel et al., 2005). Vivianite crystals and its aggregates are formed in various types of localities: in the so-called gossans, oxidation zones of iron sulphide deposits, greisenitic (Sn) and high temperature Pb-Zn ore dikes deposits. Crystals may be found also in sedimentary environment. More rarely, vivianite is present in coal deposits and in pegmatites and skarns (Bernard and Rost, 1992; Guastoni et al., 2007).

Thanks to its subtle blue colour, vivianite had been employed as a historical painting pigment. Interestingly, up to now, it has not been clearly settled whether the earthy vivianite or the ground-up vivianite crystals were used for the pigment preparation (Richter, 2007). Vivianite is a rare pigment and, so far, has been identified in only about seventy works of art. Its documented usage in Europe stretches from 1050 to 1780. The predominant countries of origin of the vivianite-containing artworks are Austria and Germany, but in the 17th century, they originated mainly in The Netherlands, including famous workshops of Rembrandt van Rijn, Aelbert Cuyp or Jan Vermeer. Other works were documented from the

Czech Republic, United Kingdom, Switzerland, Norway, Sweden and Lithuania (Richter, 2007; Castro et al., 2009; Sheldon, 2007; Karl, 2009).

In some of the artworks, the appearance of vivianite paints changed from blue to grey or yellowish brown due to vivianite's degradation (van Loon, 2008; Spring and Keith, 2009; Spring, 2001; Howard, 2003). In the mineralogical literature, vivianite is described as being prone to oxidation. There has been a discussion about its oxidation products (Ritz et al., 1974; Rodgers, 1986; Dormann et al., 1982), but the current knowledge about vivianite's oxidation series is following: vivianite (monoclinic, $\text{Fe}_3^{2+}(\text{PO}_4)_2 \cdot 8\text{H}_2\text{O}$) – metavivianite (triclinic, $\text{Fe}^{2+}\text{Fe}_2^{3+}(\text{PO}_4)_2(\text{OH})_2 \cdot 6\text{H}_2\text{O}$) – Fe^{3+} -rich "metavivianite" (triclinic with different cell dimensions) – santabarbaraite (amorphous, $\text{Fe}_3^{3+}(\text{PO}_4)_2(\text{OH})_3 \cdot 5\text{H}_2\text{O}$) (Chukanov et al., 2012). This process is accompanied by colour change: on exposition to air, white pristine vivianite quickly transforms to blue; the blue shade gradually becomes deeper and darker. Finally, vivianite changes to santabarbaraite, which is known to be yellowish brown (Pratesi et al., 2003).

There are several works describing identification of vivianite in the samples from works of art. They have been performed mainly by optical microscopy and/or scanning electron microscopy – energy dispersive spectroscopy (SEM-EDS) (Sheldon, 2007; van Loon, 2008; Spring and Keith, 2009; Karl, 2009; Howard, 2003). Spring and Keith (2009) performed also Fourier-transform infrared spectroscopy. Their results confirmed the presence of phosphate, but the bands were not enough resolved to unambiguously decide whether only vivianite, or also its degradation products/other phosphates were present.

The colour and structural changes of vivianite complicate its unambiguous identification in micro-samples of works of art. Therefore, the first paper presented in Appendix A, Čermáková et al. (2014a), focuses on comparative structural analysis of vivianite mineralogical samples and vivianite-containing micro-samples of works of art. It also deals with the suitability of vivianite for authorship studies, and covers a geological provenance study of vivianite based on its elemental composition.

Since one of the first steps in the micro-analytical procedure encompass elemental analysis by SEM-EDS, we have first focused on the provenance study of vivianite. Mineralogical samples of (meta)vivianites from various types of geological settings (Tab. 3-2) were analysed by SEM-EDS. The elemental analysis enabled the differentiation of six groups of vivianite: samples containing (i) Mn, (ii) Mn + Zn, (iii) Mg, (iv) Ca + Ti, (v) Na + Si + Al + Mg + Mn + Ca + S and (vi) no admixtures.

The samples containing manganese (viv 7 and viv 16) came from a locality of Mn-rich pegmatite (Hagendorf, GE), and a deposit of pyrite-rich graphitic shales overlaid by Mn-carbonates (Litošice, CZ). Manganese and zinc were found in the samples viv 2, viv 9 and viv 10, which all originated in the iron-ore deposits with "limonitic" (Fe-oxides and hydroxides) composition, e.g. Amberg, Germany (viv 9). Magnesium was the main minor element in samples viv 3 and viv 4, which both share the origin in sedimentary basins. Calcium and titanium were found in samples viv 8 and viv 12, which were of powdery nature and came from limestone. The group with the most diverse elemental composition (Na + Si + Al + Mg + Mn + Ca + S) comprised viv 19 and viv 20, two vivianite samples from peat bogs in the Czech Republic. Finally, no elemental admixtures were found in vivianite crystals from Wannan River, Australia, which were formed in clay underlying basalt rock exposed under the Wannan Falls.

These were the minor elemental characteristics of the studied mineralogical samples. We had the opportunity to study micro-samples of canvas paintings executed by Jean George de Hamilton (1672-1737), a painter who was active particularly in Germany, Austria and southern Bohemia. Therefore, their elemental characteristics could be compared with the mineralogical samples. The analysed micro-samples are summarised in Tab. 3-3 Part I; the paintings represent portraits of horses. Fe-P-rich grains were identified in the mixture with lead white as an underpainting of the top blue ultramarine-rich layer in the areas representing sky. For comparison, the study included also micro-sample obtained from a Late Gothic Transylvanian altarpiece, where vivianite is mixed with gypsum and, again, forms part of the underpainting.

The SEM-EDS analyses of the micro-samples showed the presence of a wide variety of elements present in the vivianite (Fe-P) grains; these included e.g. Si, Al, Mn, Na, Ca, K, Mg and S, which led to suspicion that the employed vivianite comes from peat bogs. However, one must take into account the limitations of the SEM-EDS: since the Fe-P grains were relatively small, the excitation volume mostly did exceed their dimensions, therefore, also the surrounding materials contributed to the resulting spectra. Furthermore, the preparation method of the micro-samples (embedding in resin, grinding in order to obtain cross-section) resulted in the grains' contamination. Nevertheless, it was possible to identify an element present specifically in the vivianite grains thanks to the elemental mapping: manganese (Fig. 4-1).

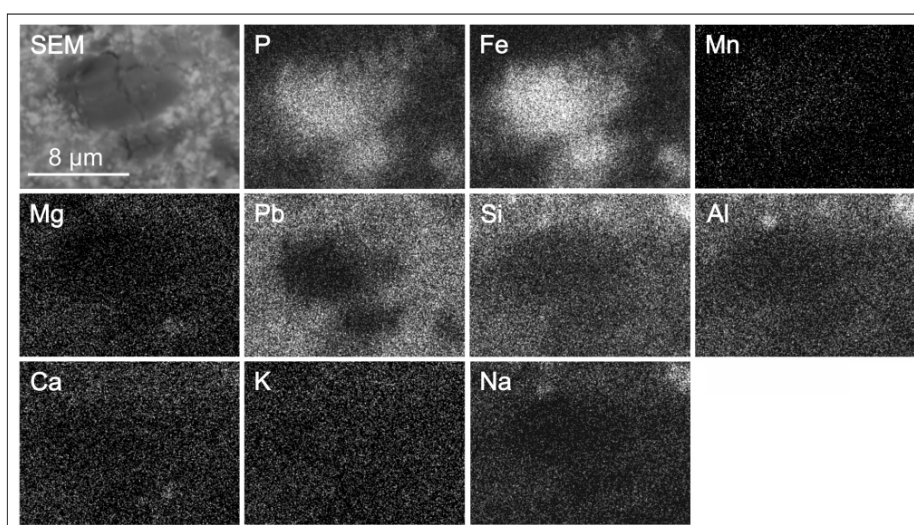


Fig. 4-1 SEM-EDS elemental mapping of micro-sample J1214-3. Mn is slightly more concentrated in the Fe-P grain, while Mg, Pb, Si, Al and Na are more concentrated in the surroundings. Ca and K do not exhibit a concentration gradient regarding the Fe-P grain. Photo: Z. Čermáková

In comparison with the mineralogical samples, the elemental composition of the micro-samples with a small amount of manganese and, probably, a certain amount of other elements like Si, Al, Na or Mg indicated sedimentary origin. This was further supported by the grains' morphology – they were mostly isometric and rather small (most often 3-7 μm). For comparison, model paint layer sample with ground-up vivianite crystals was created and its micro-sample cross-section has been observed. Indeed, the grains were larger, more angular and elongated.

After careful SEM-EDS analysis of micro-samples and detection of Fe-P rich grains, structural analysis was needed for reliable identification of vivianite. To test three types of structural methods – X-ray diffraction, Raman spectroscopy and Fourier-transform infrared

spectroscopy – on (meta)vivianite samples, we have applied them first on mineralogical samples (Tab. 3-2). For the purpose of comparison of the analytical response, we have selected sample viv 3, which was found to contain all three crystalline (meta)vivianite phases: vivianite, metavivianite and Fe³⁺-rich “metavivianite”, which were all discerned by X-ray diffraction. The presence of amorphous santabarbarite cannot be ruled out since its nature would prevent its identification by XRD.

The Fe³⁺-rich “metavivianite” is not a very-well described phase. Dormann et al. (1982) have published its X-ray diffraction pattern, but not its vibrational spectra. We were able to obtain only two types of Raman spectra on sample viv 3 – the one of partially oxidised vivianite (using 514.5 nm laser, it was possible to excite the 3479 cm⁻¹ band indicating oxidation) and the one of metavivianite as published by Chukanov et al. (2012). The FT-IR spectrum (transmission) contained bands of both vivianite and metavivianite. We have suggested that an unassigned band at approx. 1010 cm⁻¹ indicate the presence of Fe³⁺-rich “metavivianite”, however, following research of vivianite’s degradation described in the second part of this thesis revealed that this band is the first sign of vivianite’s degradation observable in its FT-IR spectrum, therefore, cannot be ascribed to Fe³⁺-rich “metavivianite”.

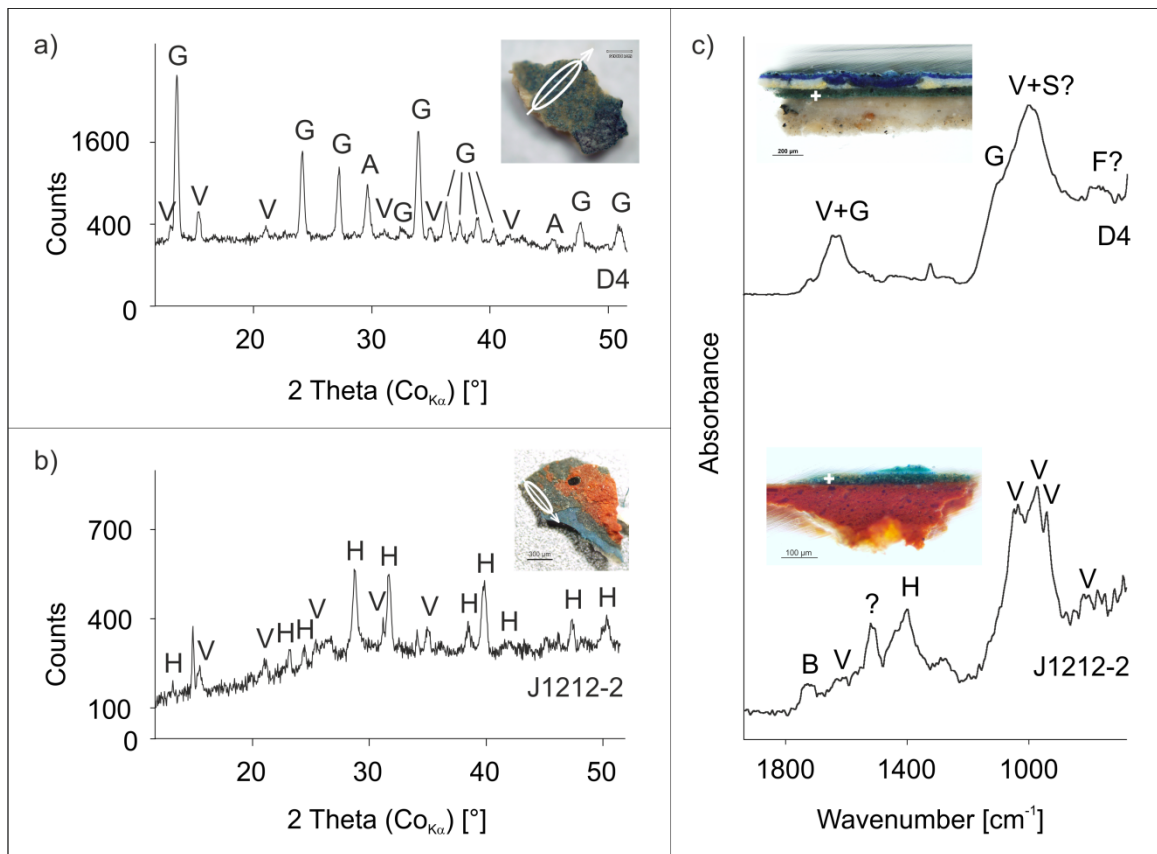


Fig. 4-2 Micro-X-ray diffraction patterns and micro-ATR micro-FT-IR spectra of micro-samples D4 and J1212-2: a) micro-XRD of fragment D4 (A=anhydrite, G=gypsum, V=vivianite); b) micro-XRD of fragment J1212-2 (H=hydrocerussite (i.e. lead white), V=vivianite); the analysed area and the incident beam direction are marked by the ellipses and the arrows, respectively, on the microphotographs of the fragments; c) micro-ATR micro-FT-IR of cross-sections D4 and J1212-2 (B=binder, F=feldspar, G=gypsum, H=hydrocerussite, S=santabarbarite, V=vivianite); white crosses in the photographs indicate the position of vivianite-rich layer. Photo: Z. Čermáková, J. Hradilová and D. Hradil

Subsequently, we have applied the structural analyses (in their micro-configurations) on micro-samples of works of art (Tab. 3-3 Part I). Micro-XRD was performed on two micro-samples (D4 and J1212-2 in the form of loose fragments) with the Fe-P rich layer sufficiently exposed for the measurement (width around 500 μm). Fig. 4-2 depicts their X-ray micro-diffraction patterns, which enabled the identification of vivianite.

If the layer is not sufficiently exposed, the methods of choice are vibrational spectroscopies, since they provide higher spatial resolution than micro-XRD. We have attempted Raman spectroscopic analysis of the micro-samples (using lasers of three different wavelengths: 514.5 nm, 633 nm and 785 nm), since the analysis of mineralogical samples showed its ability to easily discern vivianite and metavivianite. However, all the spectra were hindered by undesirable fluorescence.

Consequently, micro-FT-IR analysis in reflection mode has been performed. Unfortunately, the obtained signal to noise ratio has not been optimal, thus preventing the unambiguous identification of vivianite or its degradation products in the micro-samples. Therefore, the micro-samples were analysed by another mode of micro-FT-IR, the micro-ATR. The resulting spectra were of higher quality with better signal to noise ratio. They enabled the identification of vivianite in sample J1212-2, and their interpretation suggested the presence of vivianite and santabarbarite in sample D4 (Fig. 4-2) due to broad bands indicating the presence of amorphous phase. In the other analysed micro-samples, the spectra were either ascribed to silicates, more specifically kaolinite ($\text{Al}_2\text{Si}_2\text{O}_5(\text{OH})_4$) – J1214-3 and J1008-1, or it was not possible to define whether it is a spectrum of silicate or phosphate (J1006-1, J1009-1, J1211-1, J1213-1). The impossibility to collect the spectrum of vivianite in some of these micro-samples seems to be related to its low concentration in the respective colour layer. In that case, the detection of (meta)vivianite has to rely solely on SEM-EDS elemental analysis.

The results of structural micro-analysis clearly showed that for the identification of vivianite and its degradation products in the colour layer, micro-XRD is the method of choice if the vivianite-rich layer is sufficiently exposed on the fragment, and micro-ATR micro-FT-IR is suitable for the analysis of vivianite layers in cross-sections.

We have identified rare mineral pigment vivianite in seven canvas paintings by Jean George de Hamilton. Vivianite seems to be used consistently as an author's preference, which may be observed also in the case of Dutch Master Aelbert Cuyp – nine of his paintings with a time span from ca. 1640 to ca. 1660 were found to contain vivianite (Richter, 2007). Therefore, vivianite can be profitably used for authorship studies.

4.1.2 NATURALLY IRRADIATED FLUORITE

Fluorite has an ideal composition CaF_2 and crystallises in a cubic system. In nature, it can be found most often in the form of granular to massive aggregates or cubic crystals (Bernard and Hyršl, 2006). Dark violet-black to black variety of fluorite, which contains structural dislocations due to natural irradiation, is commonly called antozonite or fetid fluorite. When crushed, it emanates a peculiar smell, which has been only recently identified as elemental difluorine (Schmedt auf der Günne et al., 2012). Antozonite can be found e.g. in Sn-W and Sn-Cu ore veins and related greisens, Pb ore veins or fluorite-barite veins (Bernard and Hyršl, 2006). Thanks to antozonite's deep and saturated colour unrivalled by other

fluorite's colorations, antozonite has been used as a historical painting pigment (Richter et al., 2001).

Violet fluorite is a rare pigment and, so far, has been identified in only about forty works of art. In Europe, dark violet fluorite was found in artworks originating from ca. 1450 to ca. 1550 in Switzerland, Germany, throughout the Central European region (Czech Republic, Slovakia, Austria, Poland-Lower Silesia, Hungary) as well as in The Netherlands (Chlumská et al., 2010; Spring, 2007-8; Želinská, 2012; Kosinova, 2002; Spring, 2000). It seems that the usage of dark violet fluorite pigment is related with its period extraction. Šrein et al. (2010) have studied dark violet to black fluorite from several localities in the Czech Republic, Germany and Poland. They have identified Wölsendorf, Germany, as the most probable source of the antozonite pigment – it contained the highest proportion of dark-coloured grains and had been mined for silver ore from ca. 1450 to 1520-1550.

Thanks to its unique elemental composition, fluorite can be easily detected in micro-samples of works of art using SEM-EDS. However, SEM-EDS cannot display the structural damage of heavily irradiated fluorites, and structural analysis is needed. It seems that for the identification of violet fluorite pigment in micro-sample, Raman spectroscopy has been used only once (Banerjee et al., 2000). Raman spectrum of antozonite has been published by Dill and Weber (2010). However, the presented bands are not actually Raman bands of fluorite. Fluorite has a simple Raman spectrum containing one band at 322 cm^{-1} (Srivastava et al., 1971), and Dill and Weber (2010) published spectrum covering only the 400 to 2400 cm^{-1} range. X-ray diffraction studies of antozonite samples have been performed e.g. by Vlček et al. (2012) and Berman (1957). They showed that antozonites' patterns have broadened diffraction lines and the shift of their position indicates an increase of unit cell parameter in comparison to synthetic standard.

Since it is not clear whether naturally irradiated fluorite – antozonite has a specific Raman spectrum and how it potentially relates to structural damage observable by XRD, the second paper presented in Appendix A, Čermáková et al. (2014b), focuses on Raman spectroscopic and X-ray diffraction study of naturally irradiated fluorites as well as on the relation between their structural damage and colour.

Firstly, sixteen samples of naturally irradiated fluorites – antozonites as well as white synthetic standard (Tab. 3-1) were studied by X-ray diffraction. We have observed broadening of the diffraction lines (i.e. increased full-width half-maximum, FWHM) in thirteen of the studied samples; three samples (fluorite 3, 5 and 14) had FWHMs comparable to synthetic standard. The measured values of FWHM of the 111 diffraction line ranged from 0.054 (fluorite 14) to $0.114^\circ 2\text{ Theta}$ (fluorite 13).

All the studied mineralogical samples were dark-coloured; they were either violetish black or black (with one exception, viv 14 was very deep violet). When the samples were ground, the range of the observable colours significantly broadened to light violet – deep violet – violetish black – black. To objectively compare the colour (with special attention to lightness) and the structural damage indicated by diffraction patterns, UV-VIS spectrophotometry was thought to be a suitable method. It has been tested on two samples, fluorite 14 (light violet) and 16 (violetish black). Fluorite 14 exhibited one broad band with maximum positioned at approx. 580 nm, which – according to Bill and Calas (1978) – can be ascribed to the presence of calcium colloids formed due to irradiation. However, the measurement of fluorite 16 resulted in total absorption preventing the interpretation of the

spectrum. Therefore, a different approach has been taken. All sixteen ground antozonite samples were photographed under fixed conditions, each histogram has been averaged and the averages were compared with the respective FWHMs of the 111 diffraction lines. The coefficient of determination R^2 (linear regression) of the histogram averages vs. FWHMs (111) equalled to 0.7208, which is a rather strong correlation.

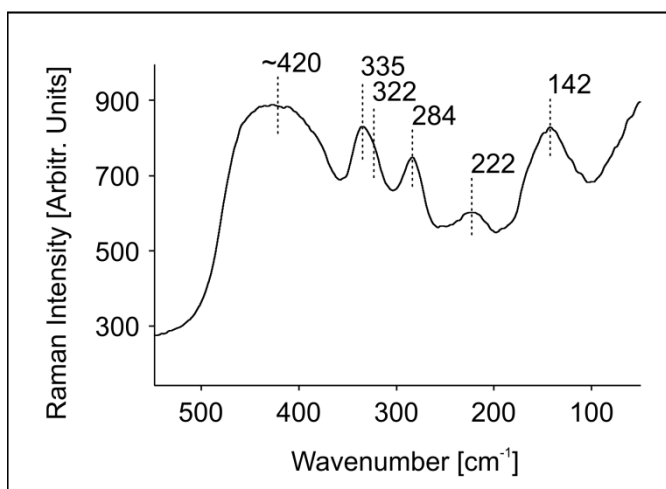


Fig. 4-3 Raman spectrum of fluorite 8 (532 nm) representing all the obtained antozonite spectra collected with 532 nm excitation

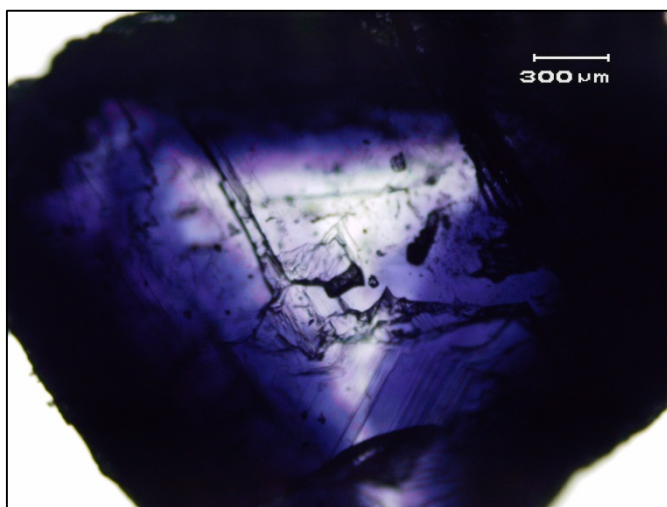


Fig. 4-4 Fragment of a crystal from fluorite 14. Photo: Z. Čermáková

We have also analysed a fragment of a crystal from fluorite 14 (Fig. 4-4), which exhibited coloration gradient from colourless to violetish black. Its Raman analysis at differently saturated areas confirmed that the intensity of the above stated five bands increase with the colour saturation.

The above-stated antozonite spectra differed from the one published by Dill and Weber (2010). Dill and Weber (2010) have recorded the spectrum using 795 nm excitation, therefore, to obtain comparable results, we have measured all the antozonite samples with the 785 nm laser. Interestingly, the spectra still differed from the one stated by Dill and

On the other hand, the reported increase of the unit cell parameter (Vlček et al., 2012) has been observed, but the correlation with the FWHM (111) values was rather poor: the R^2 was 0.6104 with the parameters calculated in HighScorePlus programme, 0.3555 for the data calculated in the ACPAR programme.

Our results show that the structural disorder of antozonites may be observed on the broadening of their diffraction lines and their decreasing lightness; on the other hand, the increase of the unit cell parameter has been observed, but is not in correlation with the increase of the diffraction lines' FWHMs.

Subsequently, all the antozonite samples as well as the synthetic standard (Tab. 3-1) were measured by Raman spectroscopy, first using 532 nm excitation. Interestingly, all the antozonite samples had almost similar spectrum with five broad bands below 500 cm^{-1} positioned at approx. 420, 335, 284, 222 and 142 cm^{-1} (Fig. 4-3). Since the only band ascribable to fluorite is located at 322 cm^{-1} (Srivastava et al., 1971), the band at 335 cm^{-1} has to be formed by two overlapping bands.

Weber (2010), but they did differ also from the ones collected with the 532 nm excitation. They contained the similarly positioned bands below 500 cm^{-1} , however, they exhibited also numerous bands above 500 cm^{-1} .

To evaluate the influence of excitation wavelength on the spectra, five selected antozonite samples from different localities (fluorite 3, 8, 13, 14, 16) and the white synthetic standard were analysed also with 445 and 633 nm excitation wavelengths. The spectra collected with the 633 nm laser were similar to the ones recorded with the 532 nm one. On the other hand, the spectra obtained with 445 nm laser still contained the bands below 500 cm^{-1} , but again as with the 785 nm laser, the spectra exhibited broad bands above 500 cm^{-1} (at different positions). The analysis by 1064 nm laser was hindered by overall fluorescence.

It seems that the antozonite-characteristic bands below 500 cm^{-1} observable in all spectra regardless of the excitation wavelength are connected with the radiation-induced damage. Poklonskaya and Khomich (2013) published Raman spectra of artificially irradiated diamonds, and similarly to antozonite, they contained numerous broad bands in the region below 500 cm^{-1} . The authors ascribe them to the local vibrations of complexes of radiation-induced point defects.

The bands above 500 cm^{-1} are of different nature. Since they can be observed only with certain excitation wavelengths, it seems that they represent fluorescence bands. The most probable explanation is that they are connected with the presence of rare earth elements (REE). Chen and Stimets (2014) observed several fluorescence bands in Dy^{3+} -doped fluorite Raman spectra excited with 785 nm in the 1000 – 2500 cm^{-1} region, and since natural fluorites are known to easily incorporate various amounts of REE (Vlček et al., 2012; Bill and Calas, 1978; Dill et al., 2011), it is highly probable that these would be manifested in their Raman spectra as well. However, it remains unclear which REE cause which fluorescence bands exhibited in the studied part of the spectra (50 – 3400 cm^{-1}). It seems probable that specific fluorescence bands may indicate specific trace elemental composition, which could be used for provenance studies. This will be a subject of further research.

To confirm that the above-described spectrum is truly specific for antozonites, three differently-coloured natural fluorite samples (bluish, green, yellow – fluorite 17, 18 and 19) were analysed by 532 and 785 nm lasers. The spectra contained a large number of broad bands, but neither of them had a spectrum similar to antozonite.

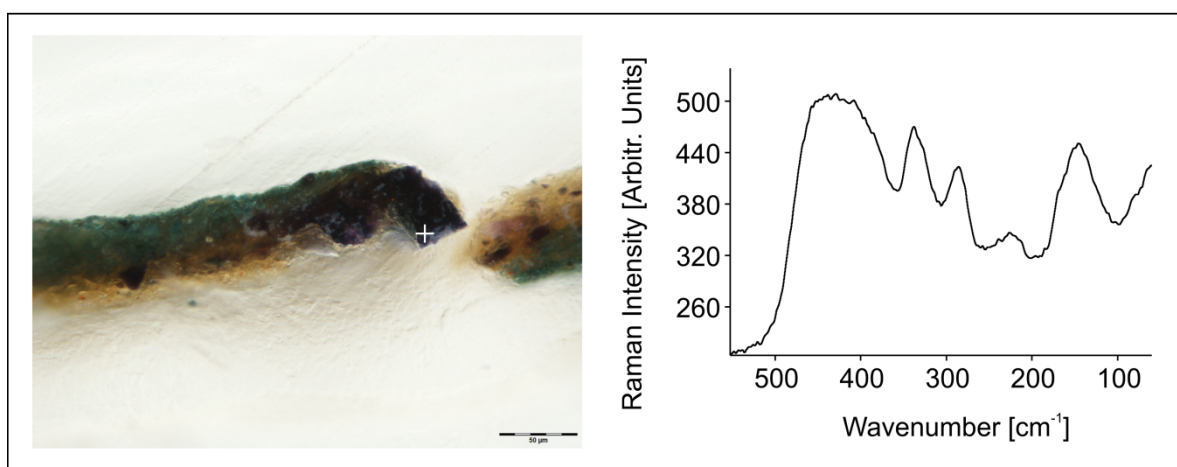


Fig. 4-5 Micro-photograph of micro-sample J1325-1hv with its Raman spectrum (532 nm). White cross indicates the analysis location. Photo: J. Hradilová

The results of the study of antozonite mineralogical samples were applied on micro-samples from works of art obtained from a Triptych with St. Jacob the Younger and St. Philip located in the Chapel of St. Wenceslaus and St. Ladislaus, Italian Court in Kutná Hora, Czech Republic, created by anonymous Master in 1497 (Tab. 3-3 Part II). First, SEM-EDS analysis enabled confirmation of the presence of fluorite grains. Then, a structural analysis was needed to study the influence of irradiation on fluorite's structure. Micro-XRD could not be applied due to thinness of the layers and insufficient accuracy of the method for reliable crystal structure calculations. Therefore, Raman spectroscopy was the method of choice. The analysis using 532 nm laser yielded antozonite spectrum with pronounced 335 cm^{-1} band indicating higher level of radiation-induced damage (Fig. 4-5). Unfortunately, the spectra collected with 785 nm excitation were hindered by fluorescence.

Interestingly, the spectrum of violet fluorite grain in paint layer of late Gothic polychromed wooden sculpture reported by Banerjee et al. (2000) is a typical fluorite spectrum with dominant 321 cm^{-1} band. It indicates that it was not the intensely-irradiated antozonite, which is corroborated by its relatively light colour.

Our results showed that Raman spectroscopy is a suitable method for identification of naturally irradiated fluorites – antozonites in micro-samples of works of art. The presented Raman spectrum may enrich the vague definition of antozonite (dark colour, specific odour during grinding), and the identification of antozonite in an artwork may lead to indications regarding the period of its creation.

4.1.3 CROCOITE

Crocoite is a lead chromate with ideal chemical formula PbCrO_4 and crystallises in a monoclinic system. It usually forms as an oxidation product of galena in basic and ultrabasic Cr-rich rocks (Bernard and Hyršl, 2006). In the form of crystals, its colour is brilliant red-orange to orange (Bernard and Hyršl, 2006); when ground, its colour ranges from yellow to orange.

Crocoite is a rare mineral and even rarer pigment. It has been identified in several Egyptian funerary artefacts (Edwards et al., 2004; Nicholson and Shaw, 2000), but its usage in European art has been reported only once, in the 13th century wall paintings under the floor of Siena Cathedral, Italy, where Mugnaini et al. (2006) confirmed its presence by micro-Raman spectroscopy. Crocoite has a synthetic counterpart, which has been frequently used as a painting pigment since the 19th century (Eastaugh et al., 2004), but the usage of natural crocoite is truly rare.

In the third paper presented in Appendix A, Hradil et al. (2014), we have reported the identification of natural crocoite in the course of a complex material research of unique 13th century wall paintings in the church of St. Gallus in Kuřívody, Czech Republic.

First, the wall paintings were analysed by portable X-ray fluorescence. The measurements indicated the presence of traditional mediaeval pigments like cinnabar (high contents of Hg in reds), orpiment and/or realgar (high contents of As in some yellows and flesh tones), Pb-based pigments (minium and/or lead white), Cu-based pigments (in greens) as well as Fe pigments (earths and ochres). Surprisingly, in the yellow parts of the paintings, also chromium has been detected, which originally raised questions about possible 19th or 20th century overpaintings. However, in this church, no such overpaintings have been documented and are not even probable from the historical point of view, taking into account

that the church was until recently in a very bad state caused among others by its usage as an ammunition or vegetable depot by the Soviet army during the occupation after 1968.

Based on the results of X-ray fluorescence, several areas were micro-sampled, including the ones with detected chromium (Tab. 3-3 Part III). The micro-samples were analysed by SEM-EDS, which identified the presence of chromium and lead in deep yellow grains (Fig. 4-6). The elemental analysis has been followed by micro-XRD; however, because the amount of these grains was rather small, no Cr-Pb containing phase could be positively identified due to the detection limit. As the most suitable method for the identification of the Cr-Pb pigment proved to be Raman spectroscopy. Fig. 4-6 depicts the obtained Raman spectrum with a dominant 844 cm^{-1} band and several low-intensity ones identifying unambiguously the Cr-Pb phase as crocoite.

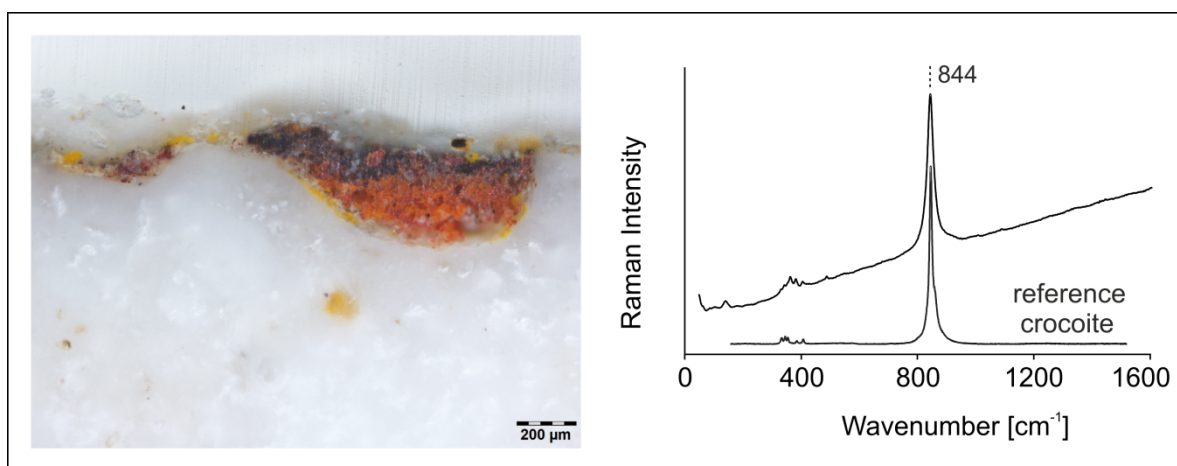


Fig. 4-6 Micro-photograph of micro-sample J1223-3 (deep yellow crocoite grains and partly darkened minium) with Raman spectrum (532 nm) obtained on one of the yellow crocoite grains. The spectrum is depicted together with crocoite reference spectrum (www.rruff.info). Photo: J. Hradilová

Our report of natural crocoite's employment as a painting pigment in Kuřívody is of utmost importance, because it is only the second report of its usage in European art. In Kuřívody, crocoite was applied in small quantities to modify the resulting hue of the dominant pigment (e.g. minium) and to highlight the outlines, which corresponds with its usage in the above-mentioned monumental wall paintings in Siena Cathedral. The creation of the Siene paintings has started around 1270 (Mugnaini et al., 2006). Therefore, the discovery of crocoite in Kuřívody supports the dating of the uncovered figural wall paintings to the end of the 13th century.

4.1.4 COPPER-BASED PIGMENTS

Copper pigments form a large group of compounds. They have a very similar elemental composition, but differ in structure. They were either extracted (natural minerals) or artificially prepared (analogues of natural minerals, organometallic compounds, synthetic pigments). In our study presented in Švarcová et al. (2014), which is the fourth paper included in Appendix A, an emphasis is put – due to the diversity of copper-based pigments – on the ones used in the European painting since Mediaeval times up to the 18th century.

The studied pigments were divided into two groups: mineral-type copper pigments (inorganic salts with mineralogical analogue), and verdigris-type copper pigments (organometallic compounds derived from copper acetate; only one of them has mineralogical analogue – hoganite).

The most wide-spread representatives of mineral-type copper pigments are copper carbonates: blue azurite ($\text{Cu}_3(\text{CO}_3)_2(\text{OH})_2$) and green malachite ($\text{Cu}_2(\text{CO}_3)(\text{OH})_2$). Apart of the carbonates, also copper chlorides and sulphates were used, even though more rarely. Among the copper chloride pigments, there is a range of structural polymorphs with identical chemical composition $\text{Cu}_2\text{Cl}(\text{OH})_3$, which comprises atacamite, paratacamite, clinoatacamite or bottalackite. The chlorides encompass also very rare pigments like indigo blue cumengeite ($\text{Pb}_{21}\text{Cu}_{20}\text{Cl}_{42}(\text{OH})_{40}\cdot 6\text{H}_2\text{O}$) or azure blue calumetite ($\text{Cu}(\text{OH},\text{Cl})_2\cdot 2\text{H}_2\text{O}$) (Scott, 2002; Švarcová et al., 2009; Švarcová et al., 2012). Copper sulphates are chemically very similar among each other and differ only by the number of hydroxyl groups and/or molecules of crystalline water: brochantite, $\text{Cu}_4\text{SO}_4(\text{OH})_6$; posnjakite, $\text{Cu}_4\text{SO}_4(\text{OH})_6\cdot \text{H}_2\text{O}$; langite, $\text{Cu}_4\text{SO}_4(\text{OH})_6\cdot 2\text{H}_2\text{O}$; or antlerite, $\text{Cu}_3\text{SO}_4(\text{OH})_4$. The variety of copper pigments is further illustrated by other rare pigments like pseudomalachite ($\text{Cu}_5(\text{PO}_4)_2(\text{OH})_4$) or chrysocolla ($\text{Cu}_{2-x}\text{Al}_x(\text{H}_{2-x}\text{Si}_2\text{O}_5)(\text{OH})_4\cdot n\text{H}_2\text{O}$ ($x < 1$)) (Scott, 2002).

Azurite has been one of the most widely used historic pigments in Mediaeval Europe up to the 17th century. In this period of time, malachite has been used as well, but not so extensively due to the availability of other green pigments on the market. In the 19th century, they were both substituted by cheaper synthetic pigments (Eastaugh et al., 2004; Scott, 2002). Copper sulphates are much rarer; posnjakite has been identified in several wall and panel paintings originating in the 15th to the 16th century as well as in the 16th century polychromy on wood (Švarcová et al., 2009; Naumova et al., 1990; Burmester and Koller, 1994), while brochantite was used in the 19th century paintings, e.g. by Portuguese painter Henrique Pousão (Correia et al., 2007). The copper chlorides of atacamite type were identified mainly in the wall paintings and in fragmentary polychromes on stone and ceramic (Švarcová et al., 2009; Naumova et al., 1990; Vandenabeele et al., 2005; Campos-Suñol et al., 2009). Chrysocolla, a rare pigment, has been detected – similarly to crocoite – in the 13th century wall paintings in Siena cathedral (Mugnaini et al., 2006).

While the mineral-type copper pigments are crystallographically well-defined, the verdigris-type pigments are, in this respect, more complicated. They can be divided into two groups – neutral and basic. The neutral verdigris, $\text{Cu}(\text{CH}_3\text{COO})_2\cdot \text{H}_2\text{O}$, mineralogically hoganite, crystallises in a monoclinic system and has a bluish green colour. Regarding the basic verdigris, Scott (2002) and Kühn (1994) published five formulas possibly available as historic pigments, however, they were not prepared phase pure and reliable reference data is missing. The only phase pure prepared basic verdigris has a following formula: $\text{Cu}_2(\text{CH}_3\text{COO})(\text{OH})_3\cdot \text{H}_2\text{O}$. It crystallises in monoclinic system and its diffraction pattern as well as infrared spectrum has been published by Švarcová et al. (2011b).

Verdigris-type compounds have been important pigments since antiquity up to the 19th century (Kühn, 1994). They were identified e.g. on Gothic panel paintings and illuminations, or on easel paintings of the 15th to the 17th century (Van Eikema Hommes, 2004).

In the presented work, we have focused primarily on the non-destructive micro-analytical procedure of copper pigments identification in micro-samples of works of art. It

has been applied on micro-samples obtained from twenty one artworks (Tab. 3-3 Part IV). The first step of the suggested procedure was careful observation under optical microscope equipped with a source of UV radiation. Copper-based pigments were used to produce blue, green and blue-green hues; under UV radiation (365 nm), they are inert – they do not exhibit any fluorescence. The second step was the analysis using SEM-EDS. This method provides elemental composition of the employed pigment and suggests the group of pigments encountered in the micro-sample. Furthermore, the analysis may reveal small and scarcely dispersed grains (e.g. Cu chlorides – in micro-samples M0412-1, M0604-2A and M0713-3), which would otherwise remained unidentified due to the detection limit of the following analytical methods (for micro-XRD typically around 2 to 5 wt. %). The third step is represented by three types of structural analysis – Raman spectroscopy, micro-FT-IR (either in reflection mode or micro-ATR) and micro-XRD.

Raman spectroscopy has been tested on three types of samples: containing Cu sulphates (M0821-1 lower green layer), Cu chlorides (J1120-1 lower green layer) and verdigris-type pigment (10-376-I-5). Since several authors encountered fluorescence when analysing blue and green compounds with 785 nm excitation (Petrová et al., 2012; Jehlička et al., 2011), 532 nm excitation wavelength was selected for this study. However, the collected spectra were still largely hindered by fluorescence. The Raman spectrum of the micro-sample M0821-1 (lower green layer) consisted of a broad fluorescence signal with just one discernible band at 978 cm^{-1} . This band could be ascribed to at least three different Cu sulphates: antlerite (985 cm^{-1}), langite (974 cm^{-1}), posnjakite (972 cm^{-1}) and possibly brochantite (990 cm^{-1}) (Martens et al., 2003). Nevertheless, Raman spectrum of a grain in the Cu-S layer led to the identification of malachite.

The Raman spectrum of micro-sample J1120-1 (lower green layer) contained a broad fluorescence signal with only one band at 3350 cm^{-1} . It could be ascribed to atacamite with a very strong vibration at 3349 cm^{-1} (Frost et al., 2002), however, it is connected with hydroxyl group, and to base the identification on one spectral feature is questionable. Therefore, even in this case Raman spectroscopy did not provide the decisive information.

The analysis of the micro-sample 10-376-I-5 was complicated by the lack of sufficient reference data. San Andrés et al. (2010) published Raman spectra of several laboratory-prepared verdigris compounds. The obtained spectrum contained several bands possibly ascribable to verdigris as presented by San Andrés et al. (2010), but it lacked the very strong band at 947 cm^{-1} (neutral verdigris) or a band at approx. similar position in case of other types of verdigris. Overall, Raman spectroscopy did not provide an unambiguous identification of copper-based pigments.

Consequently, the micro-samples were analysed using micro-FT-IR spectroscopy, first in reflection mode. The analysis provided good results; it was efficient in the identification of both copper carbonates (malachite and azurite) as well as certain sulphates. The spectrum of micro-sample M0356-6 was in very good agreement with the data published for brochantite (Makreski et al., 2005). In certain cases (e.g. M0821-1 lower green layer), the bands could be ascribed to the vibrations of the sulphate group, but the spectrum (signal to noise ratio) did not enable the specification of the sulphate (Fig. 4-7). Generally, when analysing cross-sections, the analysis was further complicated by potential signal obtained from the embedding resin, which can permeate the paint layers; fortunately, the employed polyester resin has a characteristic strong band at approx. 1270 cm^{-1} , a position where it is rare for the

pigment materials to have vibrations, therefore, its presence in the spectrum should not pass unnoticed.

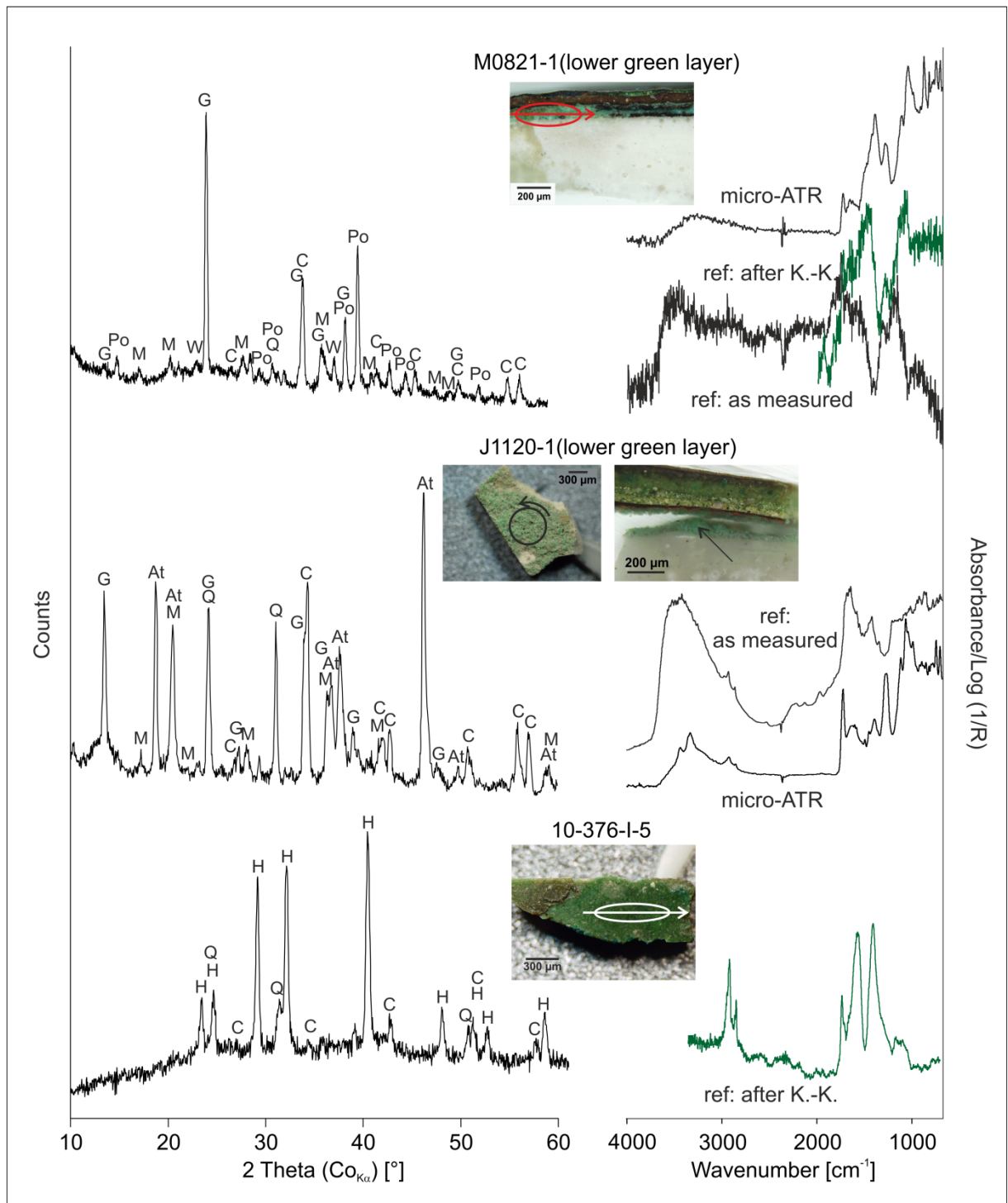


Fig. 4-7 Micro-XRD diffraction patterns and micro-FT-IR spectra of samples M0821-1 lower green layer (collected on cross-section), J1120-1 lower green layer (reflection collected on the loose fragment, micro-ATR on cross-section) and 10-376-I-5 (collected on loose fragment). Micro-XRD: the analysed area and the incident beam direction are marked by the ellipses and the arrows, respectively, on the microphotographs of the micro-samples; At=atacamite, C=calcite, G=gypsum, H=hydrocerussite, M=malachite, Po=posnjakite, Q=quartz, W=weddellite. Micro-FT-IR: ref=reflection mode, after K.-K.=after Kramers-Krönig transformation. Photo: S. Švarcová, J. Hradilová

The identification of copper chlorides is more challenging due to their usually small amount in the colour layer. However, if present as the main pigment as in the case of micro-sample J1120-1 (lower green layer), micro-FT-IR can easily detect them (Fig. 4-7).

The micro-FT-IR analysis in micro-ATR mode has been employed as well in order to compare the results with the micro-FT-IR in reflection. Micro-ATR provided much better signal to noise ratio, but surprisingly, even though the spectra collected in reflectance mode exhibited various distortions (combination of reflectance and transmission bands, “inverted” bands), the Kramers-Krönig transformation routine used to mathematically convert the results from the reflectance Log (1/R) units into Absorbance units usually led to interpretable spectra. Furthermore, the reflection mode enables analysis of loose fragments, which is beneficial if the layer to-be-analysed is exposed to a larger extent than it would be in cross-section (Fig. 4-7, compare the reflection spectra of M0821-1 (lower green layer) and J1120-1 (lower green layer) obtained on cross-section and fragment, respectively).

The micro-FT-IR analysis was efficient not only in the identification of mineral-type copper pigments, but also of the verdigris type (Fig. 4-7). Due to sometimes less-than-ideal signal to noise ratio of micro-FT-IR in reflection, an emphasis was put on the main verdigris bands related to the vibrations of the acetate group: the stretching vibration of the carboxylate group (νCOO) and, additionally, the bending vibration of the methyl group (δCH) in the case of neutral verdigris. Fig. 4-7 depicts the spectrum of verdigris obtained on micro-sample 10-376-I-5 with the position of the bands at 1577 and 1413 cm^{-1} , which correspond to the acetate group, but their position did not permit the differentiation between neutral and basic one.

Generally, micro-FT-IR provided information leading to identification of both mineral and verdigris-type copper-based pigments. Nevertheless, in certain cases, it was not able to identify specific compounds (differentiate between copper sulphates). Furthermore, the detection limits of the method is largely unknown, therefore, certain minor admixtures could pass unnoticed.

These problems can be solved by micro-XRD. In case of the micro-sample M0821-1 (lower green layer), the micro-FT-IR showed that it contains Cu sulphate, which was specified by micro-XRD to posnjakite. Pigment specification has been performed also in case of micro-sample J1120-1 (lower green layer) – to atacamite. Micro-XRD detected also the presence of malachite in both of the samples (Fig. 4-7). Micro-XRD is able to discern various polymorphs present in one sample – e.g. in the micro-sample M0424-1, three types of copper chlorides have been detected, namely atacamite, paratacamite and bottalackite.

The micro-XRD analysis of micro-sample 10-376-I-5 yielded surprising results. Even though the layer is green, the SEM-EDS analysis indicated copper and carbon and the micro-FT-IR analysis found the presence of verdigris, there were no diffraction lines ascribable to verdigris, even though copper acetates are crystalline compounds (Fig. 4-7). Verdigris was identified by micro-XRD in only one studied micro-sample: M0118-3, which originated from encaustic polychrome, i.e. the binder is wax. The other analysed samples containing verdigris (confirmed by micro-FT-IR) were bound either by oil or proteinaceous binders (like eggs) and contained also highly diffracting pigment materials like lead white or lead-tin yellow. This prompted us to perform experiments which would explain the lack of diffraction signal of verdigris in the micro-samples of works of art in these respective binders and whether the

presence of other materials influence the detection of verdigris by micro-XRD. This study will be described in the following section – Pigment Degradation Caused by Internal Agents.

In the presented work, a whole range of copper-based pigments in the micro-samples of works of art have been analysed and identified. The procedure started with careful optical microscopic observations (accompanied by UV inertness of copper pigments), followed by elemental analysis by SEM-EDS, micro-FT-IR spectroscopy either in reflection or micro-ATR mode, and finally, by micro-XRD.

4.2 PIGMENT DEGRADATION

Pigments and binders coexist for hundreds of years in paint layers of works of art. Inevitably, these heterogenous materials interact resulting in degradation, deterioration or even colour change of some of the materials. These changes may be propelled only by the composition and coexistence of the materials in the paint layer, thus caused by internal agents, or they may be initiated and driven by external agents. The main external degradative forces are represented by increased temperature, increased humidity (or its fluctuation), lighting and chemical environment (e.g. salt attack, chemicals used in the conservation/restoration procedures). This section focuses on both types of degradation.

4.2.1 CAUSED BY INTERNAL AGENTS

The changes initiated by internal agents, i.e. by the composition of materials in the paint layer, commonly take place covertly and they are not expected to be present under normal conditions. They occur even though the work of art has always been treated with care – the processes have been initiated already during the artwork's creation.

There are not many studied changes initiated by the processes within the paint layer. An example of a studied, but still not completely described and understood phenomenon, is saponification. It occurs in oil paintings with heavy-metal-containing pigments like lead white or lead-tin yellow. These interact with fatty acids in the binder, thus creating metal soaps, which crystallise, aggregate and protrude within the paint layers and may result in their flaking (Catalano et al., 2014; Osmond et al., 2012). Mazzeo et al. (2008) studied model samples naturally aged for ten years and identified the creation of not only lead-based soaps, but also the ones created with copper, manganese, cadmium and zinc.

Among the pigments which are prone to degradation via processes in the paint layers belongs also verdigris. Santoro et al. (2014) performed experiments with model samples composed of hoganite (neutral verdigris) and linseed oil. They subjected the samples to artificial ageing (increased temperature, light), although it is not known whether these conditions truly simulate actual ageing, and observed the transformation of the copper acetate bimetallic structure into monomeric species. Their primary goal was to describe the browning or darkening of verdigris, however that did not take place during their experiments. Neither browning nor darkening has been observed in the numerous studied micro-samples of works of art in the course of our research. Instead, we have encountered problems with its identification. When analysing verdigris-containing micro-samples by micro-XRD – no diffraction lines ascribable to verdigris have been detected. It contrasts with recommendations that verdigris, being a crystalline compound, should be analysed by X-ray diffraction techniques (Scott, 2002). On the other hand, it is in agreement with findings published by Van der Snickt et al. (2011), who were also not able to identify green copper pigment using XRD.

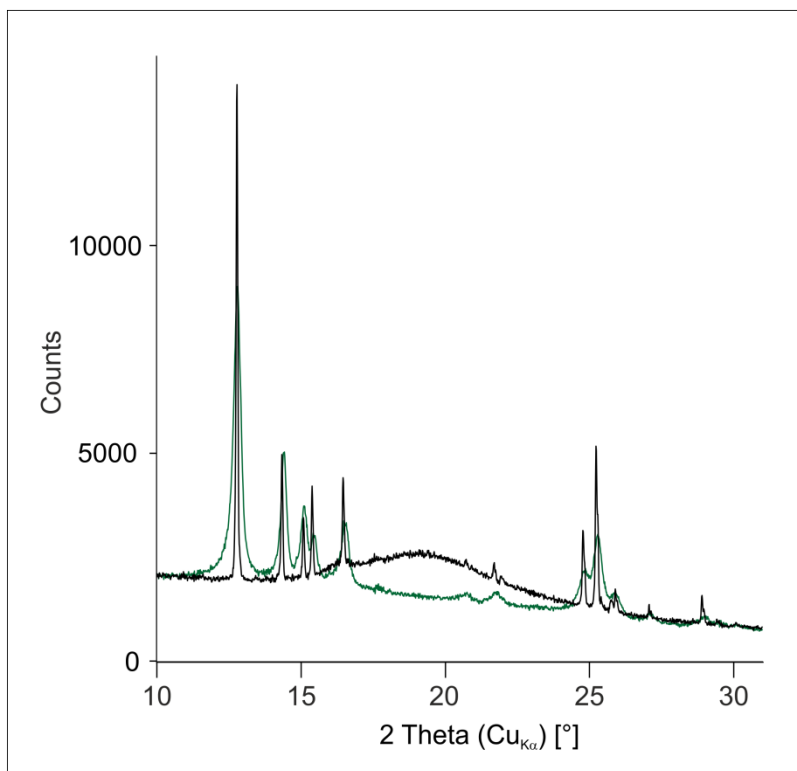


Fig. 4-8 X-ray diffraction patterns of model samples of 5 wt. % hoganite in egg yolk (black) and 5 wt. % hoganite in skin glue (green)

We have suggested that verdigris may react with oil and/or proteinaceous binders in the paint layer and, as a result, lose its crystallinity. An aspect also taken into account was the possibility that the X-ray diffraction analysis of verdigris may be influenced by highly diffracting lead containing pigments with which verdigris has been found to be mixed in the paint layers. First of all, mixtures of hoganite with lead white (PbCO_3) and lead-tin yellow (Pb_2SnO_4) were prepared in order to assess hoganite's detection limit in these mixtures. The results showed that hoganite could be identified from 2 wt. % concentration. Then, model samples of hoganite bound by proteinaceous binders – egg yolk and skin glue – were created to monitor their influence on hoganite's crystallinity, and again, assess its detection limit. X-ray diffraction measurements showed that the diffraction lines of hoganite were visible from its 5 wt. % concentration. The mixture with egg yolk did not affect hoganite's structure, in contrast with skin glue – the broadening of its diffraction lines and related decrease of crystallinity is clearly visible in Fig. 4-8. Finally, to assess the influence of both proteinaceous binders and the highly diffracting pigments, model mixtures of hoganite with equal amount of lead-tin yellow (Pb_2SnO_4) in egg and skin glue were prepared. Interestingly, in the mixture containing 5 wt. % hoganite and 5 wt. % Pb_2SnO_4 in egg, the diffraction lines of hoganite have completely disappeared. In the equivalent mixture of 5 wt. % hoganite and 5 wt. % Pb_2SnO_4 in skin glue, the hoganite's diffraction lines could be detected, but as in the previous model samples of hoganite with skin glue, the lines were broader indicating the decrease of crystallinity. The presented loss of crystallinity is in agreement with Altavilla and Ciliberto (2006), who observed the elongation of Cu-Cu and Cu-C bonds in the samples from works of art in comparison to freshly prepared model samples. It seems that the complete loss of verdigris' crystallinity is a long process which is hard to simulate. Nevertheless, our results clearly indicate the synergic effect of both the proteinaceous binders and the lead containing pigments on the possibility of verdigris detection by micro-XRD.

4.2.2 CAUSED BY EXTERNAL AGENTS

Numerous works of art have encountered less-than-ideal conditions of use and storage, or inappropriate conservation/restoration treatments. Nonetheless, even artworks

kept under normal museum conditions may show signs of degradation, commonly due to photo-sensitivity of the employed painting materials.

Several studies show that painting pigments may be sensitive to UV light, increased humidity or exposition to various salt solutions, a degradation process typical for wall paintings. Van der Snickt et al. (2009) describe the degradation of bright yellow cadmium sulfide to hydrated cadmium sulphate most probably due to light and humidity fluctuations. The degradation of lead pigments (lead white – cerussite and hydrocerussite, red lead – Pb_3O_4 and massicot, PbO) under increased humidity and in solutions with several types of salts were studied by Kotulanová et al. (2009). Švarcová et al. (2009) describe the corrosion of blue azurite into green atacamite by the action of chloride ions under the conditions of increased humidity. They also point out the importance of the presence of oxalic acid on the acceleration of the copper pigments degradation, while Castro et al. (2008) suggest that oxalic acid is present in the wall paintings as a result of excretion of certain microorganisms. Radepont et al. (2011) studied the degradation and colour change of cinnabar and its synthetic form (vermillion); they found out that it is largely affected by the presence of chloride ions and UV light. The UV irradiation also accelerates the degradation of lead chromate (synthetic crocoite), as reported by Monico et al. (2011).

The studies of pigment degradation usually do not take into account the possibility of the influence of increased temperatures on the works of art. These may be caused either by intense lighting, or a relatively common restoration/conservation technique of canvas paintings – relining, which basically consists of ironing a new canvas on the back of the old degraded one using various organic compounds (e.g. wax-resin mixtures or modern materials like BEVA 371, a complex mixture of copolymers, synthetic resin and wax) (Hackney, 2004; Ackroyd, 2002). These treatments may have harmful effect on present pigments, especially those which are prone to oxidative degradation; it is well-known that increased temperatures generally accelerate oxidation processes. That is the case of a rare mineral pigment vivianite, whose oxidation is accompanied by colour change, and it is probable that it took place in some of the works of art with reported degraded vivianite (van Loon, 2008; Spring and Keith, 2009; Howard, 2003).

Such temperature-related oxidation of vivianite may be monitored by Mössbauer spectroscopy. However, the published studies either focused on high temperatures (from 200°C up to 800°C) (Piña et al., 2010), or do not state clearly the temperature under which vivianite first starts to change (Hanzel et al., 1990). The structural changes of vivianite under increased temperatures were monitored by Tien and Waugh (1969) using X-ray diffraction (ex situ, the analysed samples were first heated, then measured), or by Poffet (2007) by high-temperature X-ray diffraction (in situ). She focused mainly on the durability of vivianite under certain temperatures, and describes the loss of intensity of the lines of vivianite diffraction pattern.

Since it is not entirely clear at which temperature vivianite starts to change, in the fifth paper included in Appendix A, Čermáková et al. (2014c), we have focused on thermal behaviour of vivianite using Mössbauer spectroscopy, high-temperature X-ray diffraction (HT-XRD) and a range of model samples and experiments including model traditional wax-resin relining in order to shed light on the temperature-related behaviour of this pigment.

The first method employed in this study was HT-XRD. We have analysed three samples with different stage of oxidation – (i) freshly laboratory-prepared vivianite, (ii)

ground vivianite crystals from Bolivia (equivalent to sample viv 10, Tab. 3-2, mixture of vivianite and metavivianite), and (iii) vivianite pigment from Kremer Pigmente (viv 2, Tab. 3-2, mixture of vivianite, metavivianite and Fe^{3+} -rich “metavivianite”). The analysis showed that a first subtle decrease of vivianite’s most intense diffraction line took place at 60°C, while at 70°C the decrease was clearly visible (Fig. 4-9). The decrease continued up to 160°C, when vivianite became completely amorphous. Interestingly, when analysing samples (ii) and (iii), at the 90°C to 110°C temperature interval, the amount of metavivianite slightly increased, then decreased similarly to vivianite. The resulting product after HT-XRD was not santabarbarite, but a different amorphous phosphate with smaller amount of water.

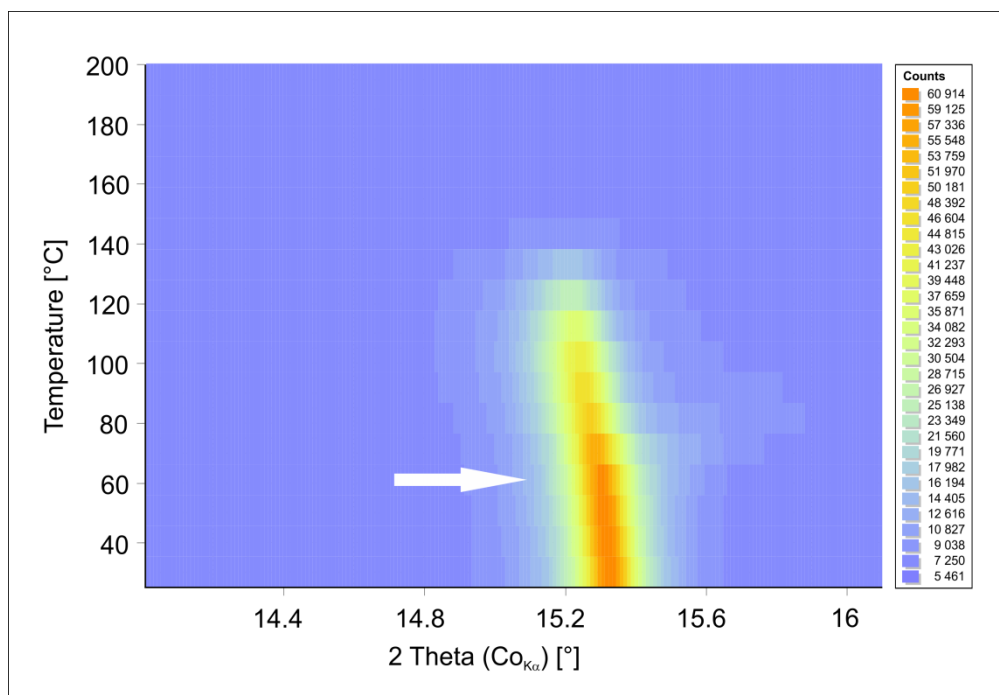


Fig. 4-9 HT-XRD pattern of synthetic vivianite depicting vivianite’s most intense diffraction line. Its “drift” to the left with increasing temperature is caused by the temperature-related expansivity of the unit cell. The white arrow indicates the first subtle decrease of vivianite’s diffraction line at 60°C

Poffet (2007) indicated fluctuation of the most intense vivianite’s diffraction line at 75°C, which contrasts with our results, which show the decrease at 70°C. The results of Piña et al. (2010) and Tien and Waugh (1969), who performed ex situ XRD measurements, did not cover the initial stages of the process; their starting temperatures were 200 and 175°C, respectively. Therefore, we have presented the first HT-XRD study covering the whole interval of vivianite’s temperature-related structure stability.

The following study of the ground natural crystals (eq. to viv 10) using Mössbauer spectroscopy showed that the amount of Fe^{3+} at room temperature was 35%. Then, the sample was heated in several steps: 60°C, 80°C, 90°C, 100°C, 110°C, 120°C and 130°C (each step lasted 30 minutes). The first observable change came after heating to 90°C, when the amount of Fe^{3+} increased to 45%. This is in agreement with the HT-XRD measurement and the observable increase of metavivianite at similar temperature. On the other hand, it contrasts with the graph published by Hanzel et al. (1990), which indicates the start of the oxidation at approx. 105°C. After heating to 130°C, the amount of Fe^{3+} reached 80%.

To monitor the changes also in the system comparable to historic paints, we have prepared several types of paint layer model samples of synthetic vivianite with four main historic binders – egg yolk, skin glue, linseed oil, water, as well as model samples composed of ground vivianite crystals (eq. to viv 10) with water to observe the behaviour of partly oxidised natural sample. The tested samples were heated again in several steps, every step took 30 minutes: 60°C, 80°C, 100°C, 120°C, 160°C and 200°C. After each step, the changes were monitored by UV/VIS spectrophotometry and optical microscopy, after every second step (80°C, 120°C and 160°C), the samples were analysed also by XRD and FT-IR in transmission mode.

After the 60°C heating step, the changes were minimal and almost imperceptible to the human eye. However, the 80°C brought visible changes. The most striking one was the change of the ground natural vivianite – from blue to greyish (Fig. 4-10). This type of colour change is an important finding, since it corresponds with the reported changes in actual works of art (van Loon, 2008; Stege et al., 2004). Both XRD and FT-IR documented its gradual amorphisation. Finally, after the 200°C heating step, the sample became bright orange.

The samples of synthetic vivianite with water and skin glue had a similar course of both the colour and the structural change to the natural ground crystals with water.

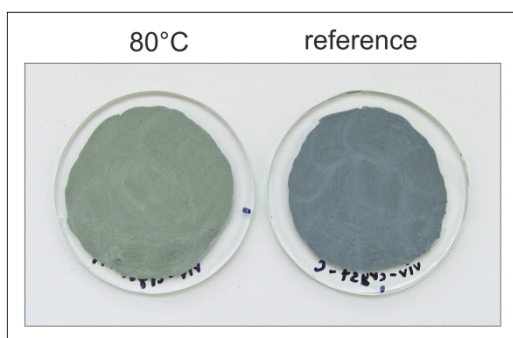


Fig. 4-10 Colour change of the ground natural vivianite after 80°C heating step together with unheated reference sample

The colour change of synthetic vivianite with egg yolk was considerably influenced by the binder. Due to the formation of combustion products, this sample became completely black after exposition to 160°C.

Synthetic vivianite prepared with linseed oil exhibited a different course of colour change than all the other samples. It was probably caused by the relative thinness of the layer, which resulted in preferential display of binder-related colour change. Nevertheless, after the 100°C heating step, optical microscopy provided an interesting insight into the influence of the binder on the vivianite pigment – vivianite grains completely surrounded

by oil became yellow, while a “lump” of aggregated vivianite grains still kept its bluish colour. Therefore, it seems that oil facilitates the transfer of heat to vivianite’s grains.

Finally, to test the effect of the common conservation/restoration treatment on canvas paintings containing vivianite, oil-on-canvas mock-ups with ground vivianite crystals pigment (eq. to viv 10) were applied with oil on a ground layer composed of iron-rich earths. One of the canvases was kept as a reference, the other one was relined in a traditional way using iron and wax-resin mixture. First, the canvas mock-up has been ironed for 10 min. under the lowest temperature possible to keep the relining process effective. The highest temperature measured from the back of the canvas by non-contact optic thermometer was 51°C, while the irreversible indicator (applied from the front of the canvas) showed that the temperature reached an interval between 54 and 60°C. After that, no colour change of the vivianite layer was observable (except the darkening of the whole mock-up due to saturation by wax-resin mixture). Consequently, the heat was applied again by ironing the canvas for 15 min. with the temperature fluctuating around 76°C. After that, the pure vivianite oil paint seemed to be slightly greyer. The analysis of RGB components of the photographs of the

pure vivianite paint before and after relining indicated darkening (by wax-resin saturation) and the loss of subtle modelling (the width of the RGB parameters decreased). A detailed study of the photographs showed that larger grains of vivianite became grey.

This was confirmed by micro-sampling of the relined and reference canvases and observation of the samples in cross-sections. The grey grain in the micro-sample after relining was analysed by Raman spectroscopy, which had the spectrum of metavivianite, while the grains in the untreated micro-sample exhibited only the spectrum of vivianite.

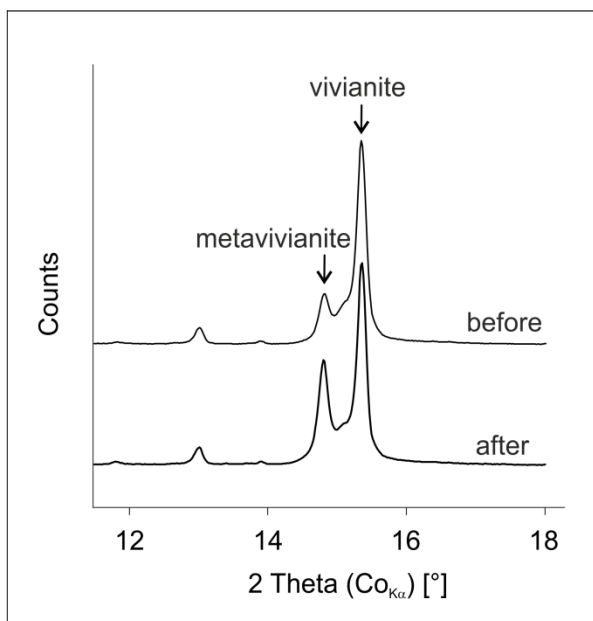


Fig. 4-11 X-ray diffraction patterns of the ground natural vivianite sample before and after the increased humidity experiment

Our results show that it is very important to properly analyse the works of art before conservation/restoration treatments and that these should be performed with care if sensitive materials like vivianite are present.

Within the range of this Ph.D. research, also preliminary experiments with the influence of increased humidity on vivianite samples have been performed with very promising results. Model paint layer samples of synthetic vivianite with water and ground natural vivianite with water were kept for three weeks in a climate chamber under room temperature and 90% relative humidity. The synthetic vivianite exhibited pronounced colour change from light blue to intense blue and first signs of degradation in its FT-IR spectrum (in transmission) – occurrence of a 1010 cm^{-1}

band, while its XRD pattern remained the same (only vivianite). The colour of the ground natural vivianite sample darkened only slightly, however, its XRD pattern showed approx. doubled amount of metavivianite compared to the state before the experiment (Fig. 4-11). These experiments will continue and, hopefully, will finally shed light on the full degradation series of vivianite, since the humidity (in contrast to temperature) seems to simulate the natural process of vivianite's oxidation.

While the temperature-related degradation processes of vivianite pigment were studied in depth, the research of a potential degradation process of orpiment is at the beginning and needs to be experimentally verified. The theoretical pathway of the degradation has been suggested in the third paper in the Appendix A, Hradil et al. (2014).

In Kuřívody, Czech Republic, the performed X-ray fluorescence measurements indicated, among others, the presence of As-rich pigments in yellow and pinkish parts of the painting. However, the As sulphides (orpiment and/or realgar) were excluded by the lack of appropriate amount of sulphur in the measurements. The following laboratory analysis using Raman spectroscopy, micro-XRD and elemental mapping by SEM-EDS proved the presence of mimetite, a hexagonal mineral with ideal chemical composition $\text{Pb}_5(\text{AsO}_4)_3\text{Cl}$. In nature, mimetite is formed as an oxidation product of galena, and is relatively rare (Bernard and Hryšl, 2006). Its rather sparse occurrence indicates that it was probably not economically

viable for exploitation. So far, mimetite's presence in works of art has been reported only twice: in the painted surface of ancient stone steles in Greece (325–275 BC) and in the painted decorations of tombs in Macedonia and Syria (2nd century AD) (Buisson et al., 2014; Eastaugh et al., 2004). We have suggested that in Kuřívody, mimetite is the degradation product of orpiment in combination with lead pigment, specifically minium.

The following process has been proposed as a possible chemical degradation pathway of orpiment in combination with minium: since the environment in wall paintings is alkaline due to the lime-based plasters, orpiment becomes less stable and tends to dissolve to thioarsenites (AsS_3)₃ and arsenites (AsO_3)₃ (Darban et al., 2011). The oxidation of trivalent arsenic to thioarsenates (AsS_4)₃ and arsenates (AsO_4)₃ could take place under the action of atmospheric oxygen. While on other places of the paintings, minium was found to be darkened due to formation of plattnerite (see Fig. 4-6) in accordance with already published data regarding its degradation (Kotulanová et al., 2009), in combination with orpiment, its degradation pathway would be modified. Minium would be preferentially reduced to Pb^{2+} ions and, simultaneously, arsenolite (As_2O_3) and elemental sulphur would form. Subsequently, increased activity of dissolved chloride ions under increased humidity and alkaline conditions would lead to formation of lead chloroarsenates like mimetite.

However, this process has been suggested only theoretically, and a profound study encompassing experimental laboratory work is needed to elucidate the occurring degradation phenomena.

5. CONCLUSIONS

The micro-analytical and provenance/authorship studies of mineral painting pigments brought the following findings:

- for the identification of vivianite and its degradation products in the paint layer, the structural analysis of choice is micro-XRD if the vivianite-rich layer is sufficiently exposed on the fragment, and micro-ATR micro-FT-IR is suitable for the analysis of vivianite layers in cross-sections;
- vivianite has been identified in seven paintings by Jean George de Hamilton, seems to be used consistently by the author and, therefore, is suitable for authorship ascription;
- the comparative elemental study of mineralogical samples and the micro-samples of works of art as well as of the grain morphology indicate sedimentary origin of the vivianite pigment in the de Hamilton's works;
- the structural disorder of antozonite samples may be observed on the broadening of their diffraction lines and their decreasing lightness, but the observed increase of the unit cell parameter is not in correlation with the increase of the diffraction lines' FWHMs;
- antozonite has a specific Raman spectrum, which enriches its rather vague definition; it can be profitably used for its identification in micro-samples of works of art, thus indicating the period of the artwork creation due to restricted historical extraction;
- an extremely rare natural mineral pigment crocoite has been identified in unique wall paintings in St. Gallus church in Kuřívody; it is only a second report of its usage in European art and corroborates the dating of the paintings to the end of the 13th century;
- a micro-analytical procedure of copper-based pigments' identification in paint layer has been elaborated and tested on numerous micro-samples of artworks; it is effective for both mineral-type and verdigris-type pigments.

Pigment degradation, either caused by internal or external agents, has been studied on various types of model samples and experiments. It was found that:

- hoganite loses crystallinity in proteinaceous binders (esp. skin glue); its detection in the paint layer is further hindered by the presence of highly diffracting pigments like lead white or lead-tin yellow;
- vivianite is sensitive to increased temperatures (already 70°C initiates its amorphisation as indicated by HT-XRD) and its oxidation started after heating to 90°C; exposition to 80°C caused pronounced colour change from blue to grey, a degradation described in actual works of art – model experiments showed that these could be caused by relining;
- a potential degradation pathway of orpiment in the presence of lead-based pigments in wall paintings has been theoretically proposed; further experimental work is needed for its verification.

6. REFERENCES

- Ackroyd, P. (2002) The structural conservation of canvas paintings: changes in attitude and practice since the early 1970s. *Rev. Conserv.* 3: 3-14
- Altavilla, C., Ciliberto, E. (2006) Copper resinate: an XPS study of degradation. *Appl. Phys. A* 83:699-703
- Ambers, J. (2004) Raman analysis of pigments from the Egyptian Old Kingdom. *J. Raman Spectrosc.* 35:768-773
- Andalò, C., Bicchieri, M., Bocchini, P., Casu, G., Galletti, G. C., Mandò, P. A., Nardone, M., Sodo, A., Plossi Zappalà, M. (2001) The beautiful “Trionfo d’Amore” attributed to Botticelli: a chemical characterisation by proton-induced X-ray emission and micro-Raman spectroscopy. *Anal. Chim. Acta* 429:279-286
- Arnold, D. E., Bohor, B. F., Neff, H., Feinman, G. M., Williams, P. R., Dussubieux, L., Bishop, R. (2012) The first direct evidence of pre-columbian sources of palygorskite for Maya Blue. *J. Archaeol. Sci.* 39:2252-2260
- Bacci, M., Picollo, M., Trumpy, G., Tsukada, M., Kunzelman, D. (2007) Non-invasive identification of white pigments on 20th-century oil paintings by using fiber optic reflectance spectroscopy. *J. Am. Inst. Conserv.* 46:27-37
- Banerjee, A., Nasdala, L., Wähning, A. (2000) Identification of violet fluorite on a Late Gothic wooden sculpture by means of high-resolution Raman spectroscopy. [in German] *Arbeitsblätter für Restauratoren* 33:243-246
- Beck, L., Rousseliere, H., Castaing, J., Duran, A., Lebon, M., Moignard, B., Plassard, F. (2014) First use of portable system coupling X-ray diffraction and X-ray fluorescence for in-situ analysis of prehistoric rock art. *Talanta* 129:459-464
- Bernard, J. H., Rost, R. (1992) Encyclopaedia of minerals. [in Czech] Academia, Prague
- Bernard, J. H., Hyršl, J. (2006) Minerals and their localities, Granit, Prague
- Berman, R. (1957) Some physical properties of naturally irradiated fluorite. *Am. Mineral.* 42:191-203
- Bill, H., Calas, G. (1978) Color centers, associated rare-earth ions and the origin of coloration in natural fluorites. *Phys. Chem. Minerals* 3:117-131
- Boissonnas, P. B., Diethelm A. K. (1981) Some problems affecting choice, formulation and application of materials in restoration and lining. Paris: International Council of Museums. In: 6th Triennial Meeting/ICOM Committee for Conservation, Ottawa, 21-25 September, 1981

Bonizzoni, L., Bruni, S., Guglielmi, V., Milazzo, M., Neri, O. (2011) Field and laboratory multi-technique analysis of pigments and organic painting media from an Egyptian coffin (26th dynasty). *Archaeometry* 53:1212-1230

Buisson, N., Burlot, D., Eristov, H., Eveno, M., Sarkis, N. (2014) The Tomb of the Three Brothers in Palmyra: The Use of Mimetite, A Rare Yellow Pigment, in A Rich Decoration. *Archaeometry*, DOI: 10.1111/arcm.12087

Burmester, A., Koller, J. (1994) Der heilige Alexius: naturwissenschaftliche Untersuchung der Farbfassung Hans Burgkmairs, In: Der heilige Alexius im Augsburger Maximilianmuseum, Arbeitsheft 67, Bayerisches Landesamt Für Denkmalpflege, Munich, 38-47

Campos-Suñol, M. J., De la Torre-Lopez, M. J., Ayora-Cañada, M. J., Dominguez-Vidal, A. (2009) Analytical study of polychromy on exterior sculpted stone. *J. Raman Spectrosc.* 40:2104-2110

Castro, K., Sarmiento, A., Martínez-Arkarazo, I., Madariaga, J. M., Fernández, L. A. (2008) Green Copper Pigments Biodegradation in Cultural Heritage: From Malachite to Moolooite, Thermodynamic Modeling, X-ray Fluorescence, and Raman Evidence. *Anal. Chem.* 80:4103-4110

Castro, S., Reden, A., von Baumer, U., Dietemann, P., Stege, H., Fiedler, I., Tilenschi, C., Klaas, J. (2009) Examinations of two 17th century Dutch paintings with respect to colour alteration and the greyish appearance of the paint layers. *Zeitschrift für Kunsttechnologie und Konservierung* 23:177-195

Catalano, J., Yao, Y., Murphy, A., Zumbulyadis, N., Centeno, S. A., Dybowski, C. (2014) Nuclear Magnetic Resonance Spectra and Pb-207 Chemical-Shift Tensors of Lead Carboxylates Relevant to Soap Formation in Oil Paintings. *Appl. Spectrosc.* 68:280-286

Chen, H., Stimets, R. W. (2014) Fluorescence of trivalent neodymium in various materials excited by a 785 nm laser. *Am. Mineral.* 99:332-342

Chlumská, Š., Pechová, D., Šefců, R., Třeštíková, A. (2010) Examples of the use of fluorite in painting and sculpture of the late Gothic and early Renaissance in the historical art funds of Bohemia and Moravia; results of the partial investigation of selected works. Proceedings of the 3rd Interdisciplinary Conference of ALMA held in Prague, 24-25 Nov, *Acta Artis Academica*: 165-168, Academy of Fine Arts in Prague, Prague

Chukanov, N. V., Scholz, R., Aksenov, S. M., Rastsvetaeva, R. K., Pekov, I. V., Belakovskiy, D.I., Krambrock, K., Paniago, R. M., Righi, A., Martins, R. F., Belotti, F. M., Bermanec, V. (2012) Metavivianite, $\text{Fe}^{2+}\text{Fe}^{3+}_2(\text{PO}_4)_2(\text{OH})_2 \cdot 6\text{H}_2\text{O}$: new data and formula revision. *Mineral. Mag.* 76:725-741

Clark, R. J. H., Hrak, R. R., Salvadó, N., Butí, S., Pradell, T. (2010) Spectroscopy study of mural paintings from the Pyrenean Church of Saint Eulàlia of Unha. *J. Raman Spectrosc.* 41:1418-1424

- Clementi, C., Ciocan, V., Vagnini, M., Doherty, B., Tabasso, M. L., Conti, C., Brunetti, B. G., Miliani, C. (2011) Non-invasive and micro-destructive investigation of the Domus Aurea wall painting decorations. *Anal. Bioanal. Chem.* 401:1815-1826
- Correia, A. M., Clark, R. J. H., Ribeiro, M. I. M., Duarte, M. L. T. S. (2007) Pigment study by Raman microscopy of 23 paintings by the Portuguese artist Henrique Pousão (1859–1884). *J. Raman Spectrosc.* 38:1390-1405
- Cristini, O., Kinowski, C., Turrell, S. (2010) A detailed micro-Raman spectroscopic study of wall paintings of the period AD 100 – 200: effect of atmospheric conditions on the alteration of samples. *J. Raman Spectrosc.* 41:1410-1417
- Darban, A. K., Aazami, M., Meléndez, A. M., Abdollahy, M., Gonzalez, I. (2011) Electrochemical study of orpiment (As_2S_3) dissolution in a NaOH solution. *Hydrometallurgy* 105:296-303
- David, A. R., Edwards, H. G. M., Farwell, D. W., De Faria, D. L. A. (2001) Raman spectroscopic analysis of ancient Egyptian pigments. *Archaeometry* 43:461-473
- De Benedetto, G. E., Fico, D., Margapoti, E., Pennetta, A., Cassiano, A., Minerva, B. (2013) The study of the mural painting in the 12th century monastery of Santa Maria delle Cerrate (Puglia-Italy): characterization of materials and techniques used. *J. Raman Spectrosc.* 44:899-904
- Dill, H. G. (2009) The Hagendorf-Pleystein phosphate pegmatites (NE Bavaria, Germany) – a mineralogical, chronological and sedimentological overview. *Estudos Geológicos* 19:117-120
- Dill, H. G., Weber, B. (2010) Accessory minerals of fluorite and their implication regarding the environment of formation (Nabburg-Wölsendorf fluorite district, SE Germany), with special reference to fetid fluorite ("Stinkspat"). *Ore Geol. Rev.* 37:65-86
- Dill, H. G., Hansen, B. T., Weber, B. (2011) REE contents, REE minerals and Sm/Nd isotopes of granite- and unconformity-related fluorite veins at Nabburg-Wölsendorf, SE Germany. *Ore Geol. Rev.* 40:132–148
- Dormann, J.-L., Gaspérin, M., Poullen, J.-F. (1982) Étude structurale de la séquence d'oxydation de la vivianite $Fe_3(PO_4)_2 \cdot 8H_2O$. *Bull. Mineral.* 105:147-160
- Eastaugh, E., Walsh, V., Chaplin, T., Siddal, R. (2004) *The Pigment Compendium – A Dictionary of Historical Pigments*. Elsevier, Amsterdam
- Edwards, H. G. M., Villar, S. E. J., Eremin, K. A. (2004) Raman spectroscopic analysis of pigments from dynastic Egyptian funerary artefacts. *J. Raman Spectrosc.* 35:786-795
- Fagel, N., Alleman, L. Y., Granina, L., Hatert, F., Thamo-Bozso, E., Cloots, R., André, L. (2005) Vivianite formation and distribution in Lake Baikal sediments. *Global Planet Change* 46:315-336

Franquelo, M. L., Duran, A., Castaing, J., Arquillo, D., Perez-Rodriguez, J. L. (2012) XRF, μ -XRD and μ -spectroscopic techniques for revealing the composition and structure of paint layers on polychrome sculptures after multiple restorations. *Talanta* 89:462-469

Frost, R., Martens, W., Kloprogge, T., Williams, P. (2002) Raman spectroscopy of the basic copper chloride minerals atacamite and paratacamite - implications for the study of copper, brass and bronze objects of archeological significance. *J. Raman Spectrosc.* 33:801-806

Guastoni, A., Nestola, F., Mazzoleni, G., Vignola, P. (2007) Mn-rich graffonite, ferrisicklerite, stanekite and Mn-rich vivianite in a granitic pegmatite at Soe Valley, central Alps, Italy. *Mineral. Mag.* 71:579-585

Hackney, S. (2004) Paintings on canvas: lining and alternatives. *Tate Papers* 2

Hanzel, D., Meisel, W., Hanzel, D., Gütlich, P. (1990) Mössbauer effect study of the oxidation of vivianite. *Solid State Commun.* 76:307-310

Howard, H. (2003) Pigments of English Medieval Wall Painting. Archetype Publications, London

Hradil, D., Píšková, A., Hradilová, J., Bezdička, P., Lehrberger, G., Gerzer, S. (2011) Mineralogy of Bohemian green earth pigment and its microanalytical evidence in historical paintings. *Archaeometry* 53:563-586

Hradilová, J. (2013) Interpretation of the painting technique supported by material research. In: Hradil, D., Hradilová, J., Fogaš, I., Hrdličková Kučková, Š.: Contribution of material analyses to interpretation of the painting technique and art historical research in general [in Czech with English extended abstracts], Academy of Fine Arts in Prague, Prague, 17-27

Iriarte, E., Foyo, A., Sanchez, M. A., Tomillo, C., Setien, J. (2009) The origin and geochemical characterization of red ochres from the Tito Bustillo and Monte Castillo caves (Northern Spain). *Archaeometry* 51:231-251

JCPDS PDF-2 database, International Centre for Diffraction Data, Newtown Square, PA, U.S.A. release 54, 2004

Jehlička, J., Culka, A., Vandenabeele, P., Edwards, H. G. M. (2011) Critical evaluation of a handheld Raman spectrometer with near infrared (785 nm) excitation for field identification of minerals. *Spectrochim. Acta, Part A* 80:36-40

Karl, D. (2009) Technological examination of the romanesque triumph-crucifix from the Holy cross church in Klöden, *Zeitschrift für Kunsttechnologie und Konservierung* 23:140-159

Kratochvíl, J. (1961) Topographic mineralogy of Bohemia IV (L-N). [in Czech] Nakl. Československé akademie věd, Prague

Klaproth, M. H. (1807) Chemische Untersuchung der Blau-Eisenerde, von Eckartsberg. In: Beiträge zur Chemischen Kenntniss der Mineralkörper. Decker and Co., Posen and Heinrich August Rottmann, Berlin, 120-122

Kosinova, A. (2002) From first aid to fluorite: Identification of a rare purple pigment. *V&A Conservation Journal* 42:6-8

Košařová, V., Hradil, D., Němec, I., Bezdička, P., Kanický, V. (2013) Microanalysis of clay-based pigments in painted artworks by the means of Raman spectroscopy. *J. Raman Spectrosc.* 44:1570-1577

Kotulanová, E., Bezdička, P., Hradil, D., Hradilová, J., Švarcová, S., Grygar, T. (2009) Degradation of lead-based pigments by salt solutions. *J. Cult. Herit.* 10:367-378

Kühn, H. (1994) In: Roy A. (Ed.) Artists' Pigments: A Handbook of Their History and Characteristics Vol. 2, Oxford University Press, Oxford

Larkin, P. J. (2011) Infrared and Raman spectroscopy: principles and spectral interpretation. Elsevier, Waltham/San Diego/Oxford/Amsterdam

Lichvár, P., Liška, M., Galusek, D. (2002) What is the true Kramers-Krönig transform? *Ceramics – Silikáty* 46:25-27

Mahmoud, H. H. M. (2012) Microanalysis of blue pigments from the Ptolemaic temple of Hathor (Thebes), Upper Egypt: a case study. *Surf. Interface Anal.* 44:1271-1278

Makreski, P., Jovanovski, G., Dimitrovska, S. (2005) Minerals from Macedonia XIV. Identification of some sulfate minerals by vibrational (infrared and Raman) spectroscopy. *Vib. Spectrosc.* 39:229-239

Martens, W., Frost, R. L., Kloprogge, J. T., Williams, P. A. (2003) Raman spectroscopic study of the basic copper sulphates – implications for copper corrosion and "bronze disease". *J. Raman Spectrosc.* 34:145-151

Mass, J., Sedlmair, J., Schmidt Patterson, C., Carson, D., Buckley, B., Hirschmugl, C. (2013) SR-FTIR imaging of the altered cadmium sulfide yellow paints in Henri Matisse's *Le Bonheur de vivre* (1905 – 6) – examination of visually distinct degradation regions. *Analyst* 138:6032-6043

Mattei, E., de Vivo, G., de Santis, A., Gaetani, C., Pelosi, C., Santamaria, U. (2008) Raman spectroscopic analysis of azurite blackening. *J. Raman Spectrosc.* 39:302-306

Mattievich, E., Danon, J. (1977) Hydrothermal synthesis and Mössbauer studies of ferrous phosphates of the homologous series $\text{Fe}_3^{2+}(\text{PO}_4)_2(\text{H}_2\text{O})_n$. *J. Inorg. Nucl. Chem.* 39:569-580

Mazzeo, R., Joseph, E., Prati, S., Millemaggi, A. (2007) Attenuated Total Reflection–Fourier transform infrared microspectroscopic mapping for the characterisation of paint cross-sections. *Anal. Chim. Acta* 599:107-117

Mazzeo, R., Prati, S., Quaranta, M., Joseph, E., Kendix, E., Galeotti, M. (2008) Attenuated total reflection micro FTIR characterisation of pigment-binder interaction in reconstructed paint films. *Anal. Bioanal. Chem.* 392:65-76

Miguel, C., Claro, A., Gonçalves, A. P., Muralha, V. S. F., Melo, M. J. (2009) A study on red lead degradation in a medieval manuscript Lorvão Apocalypse (1189). *J. Raman Spectrosc.* 40:1966-1973

Mineralogical database (1993-2013) Jolyon Ralph and Ida Chau; information on Anloua, Cameroon. <http://www.mindat.org/loc-55149.html> Accessed 18 Jan 2013

Monico, L., Van der Snickt, G., Janssens, K., De Nolf, W., Miliani, C., Verbeeck, J., Tian, H., Tan, H., Dik, J., Radepont, M., Cotte, M. (2011) Degradation Process of Lead Chromate in Paintings by Vincent van Gogh Studied by Means of Synchrotron X-ray Spectromicroscopy and Related Methods. 1. Artificially Aged Model Samples. *Anal. Chem.* 83:1214-1223

Mugnaini, S., Bagnoli, A., Bensi, P., Droghini, F., Scala, A., Guasparri, G. (2006) Thirteenth century wall paintings under the Siena Cathedral (Italy). Mineralogical and petrographic study of materials, painting techniques and state of conservation. *J. Cult. Herit.* 7:171-185

Naumova, M. M., Pisareva, S. A., Nechiporenko, G. O. (1990) Green copper pigments of old Russian frescoes, *Stud. Conserv.* 35:81-88

Nel, P., Lau, D., Hay, D., Wright, N. (2006) Non-destructive micro-X-ray diffraction analysis of painted artefacts: Determination of detection limits for the chromium oxide–zinc oxide matrix. *Nucl. Instrum. Methods Phys. Res., Sect. B* 251:489-495

Nicholson, P. T., Shaw, I. (2000) *Ancient Egyptian Materials and Techniques*. Cambridge University Press, New York

Olivares, M., Castro, K., Corchón, M. S., Gárate, D., Murelaga, X., Sarmiento, A., Etxebarria, N. (2013) Non-invasive portable instrumentation to study Palaeolithic rock paintings: the case of La Peña Cave in San Roman de Candamo (Asturias, Spain). *J. Archaeol. Sci.* 40:1354-1360

Osmond, G., Boon, J. J., Puskar, L., Drennan, J. (2012) Metal Stearate Distributions in Modern Artists' Oil Paints: Surface and Cross-Sectional Investigation of Reference Paint Films Using Conventional and Synchrotron Infrared Microspectroscopy. *Appl. Spectrosc.* 66:1136-1144

Pagès-Camagna, S., Laval, E., Vigears, D., Duran, A. (2010) Non-destructive and in situ analysis of Egyptian wall paintings by X-ray diffraction and X-ray fluorescence portable systems. *Appl. Phys. A* 100:671-681

- Perez-Rodriguez, J. L., Robador, M. D., Centeno, M. A., Siguenza, B., Duran, A. (2014) Wall paintings studied using Raman spectroscopy: A comparative study between various assays of cross sections and external layers. *Spectrochim. Acta, Part A* 120:602-609
- Petrová, Z., Jehlička, J., Čapoun, T., Hanus, R., Trojek, T., Goliáš, V. (2012) Gemstones and noble metals adorning the sceptre of the Faculty of Science of Charles University in Prague: integrated analysis by Raman and XRF handheld instruments. *J. Raman Spectrosc.* 43:1275-1280
- Pérez-Arategui, J., Pardosa, C., Abad, J.-L., García, J.-R. (2013) Microcharacterization of a Natural Blue Pigment Used in Wall Paintings During the Romanesque Period in Northern Spain. *Microsc. Microanal.* 19:1645-1652
- Pięta, E., Proniewicz, E., Szmelter-Fausek, B., Olszewska-Świetlik, J., Proniewicz, L. M. (2014) Micro-Raman spectroscopy analysis of the 17th century panel painting 'Servilius Appius' by Isaac van den Blocke. *J. Raman Spectrosc.* In Press. DOI 10.1002/jrs.4489
- Piña, C., Arriola, H., Nava, N. (2010) Mössbauer spectroscopy of iron phosphate $\text{Fe}_3(\text{PO}_4)_2(\text{H}_2\text{O})_n$ pigments. *J. Phys.: Conf. Ser.* 217:1-4
- Pitarch, A., Ramon, A., Alvarez-Perez, A., Castro, K., Madariaga, J. M., Queralt, I. (2014) Multispectroscopic Characterization of Oil on Copper Painting. *Spectrosc. Lett.* 47:38-51
- Poffet, M. S. (2007) Thermal runaway of the dried sewage sludge in the storage tanks: from molecular origins to technical measures of smouldering fire prevention. Dissertation, Faculty of Science, University of Fribourg, Fribourg
- Poklonskaya, O. N., Khomich, A. A. (2013) Raman scattering in a diamond crystal implanted by high-energy nickel ions. *J. Appl. Spectrosc.* 80:715-720
- Pratesi, G., Cipriani, C., Giuli, G., Birch, W. D. (2003) Santabarbaraitite: a new amorphous phosphate mineral. *Eur. J. Mineral.* 15:185-192
- Prati, S., Joseph, E., Sciutto, G., Mazzeo, R. (2010) New Advances in the Application of FTIR Microscopy and Spectroscopy for the Characterization of Artistic Materials. *Acc. Chem. Res.* 43:792-801
- Radepont, M., de Nolf, W., Janssens, K., Van der Snickt, G., Coquinot, Y., Klaassen, L., Cotte, M. (2011) The use of microscopic X-ray diffraction for the study of HgS and its degradation products corderoite ($\alpha\text{-Hg}_3\text{S}_2\text{Cl}_2$), kenh suite ($\gamma\text{-Hg}_3\text{S}_2\text{Cl}_2$) and calomel (Hg_2Cl_2) in historical paintings. *J. Anal. At. Spectrom.* 26:959-968
- Richter, M., Hahn, O., Fuchs, R. (2001) Purple Fluorite: A Little Known Artists' Pigment and Its Use in Late Gothic and Early Renaissance Painting in Northern Europe. *Stud. Conserv.* 46:1-13

Richter, M. (2007) Shedding some new light on the blue pigment 'vivianite' in technical documentary sources of northern Europe. *Art Matters, Netherlands Technical Studies in Art* 4:37-53

Ritz, C., Essene, E. J., Peacor, D. R. (1974) *Am. Mineral.* 59:896-899

Rodgers, K. A. (1986) Metavivianite and kerchenite: a review. *Mineral. Mag.* 50:687-691

Rodríguez, A., Eremin, K., Khandekar, N., Stenger, J., Newman, R., Bazeta, F., Escohotado, M. T. (2010) Characterization of calcium sulfate grounds and fillings of applied tin-relief brocades by Raman spectroscopy, Fourier transform infrared spectroscopy, and scanning electron microscopy. *J. Raman Spectrosc.* 41:1517-1524

Salvant Plisson, J., de Viguerie, L., Tahroucht, L., Menu, M., Ducouret, G. (2014) Rheology of white paints: How Van Gogh achieved his famous impasto. *Colloids Surf., A* 458:134-141

Samain, L., Grandjean, F., Long, G. J., Martinetto, P., Bordet, P., Sanyová, J., Strivay, D. (2013) Synthesis and fading of eighteenth-century Prussian blue pigments: a combined study by spectroscopic and diffractive techniques using laboratory and synchrotron radiation sources. *J. Synchrotron Radiat.* 20:460-473

San Andrés, M., de la Roja, J. M., Baonza, V. G., Sancho, N. (2010) Verdigris pigment: a mixture of compounds. Input from Raman spectroscopy. *J. Raman Spectrosc.* 41:1468-1476

Santoro, C., Zarkout, K., Le Ho, A. S., Mirambet, F., Gourier, D., Binet, L., Pages-Camagna, S., Reguer, S., Mirabaud, S., Le Du, Y., Griesmar, P., Lubin-Germain, N., Menu, M. (2014) New highlights on degradation process of verdigris from easel paintings. *Appl. Phys. A: Mater. Sci. Process.* 114:637-645

Scott, D. A. (2002) *Copper and Bronze in Art – Corrosion, Colorants, Conservation.* Getty Publications, Los Angeles

Schmedt auf der Günne, J., Mangstl, M., Kraus, F. (2012) Occurrence of Difluorine F₂ in Nature – In Situ Proof and Quantification by NMR Spectroscopy. *Angew. Chem., Int. Ed.* 51:7847-7849

Sheldon, L. (2007) Blue and yellow pigments – the hidden colours of light in Cuyp and Vermeer. *Art Matters, Netherlands Technical Studies in Art* 4:97-102

Smith, G. D., Burgio, L., Firth, S., Clark, R. J. H. (2001) Laser-induced degradation of lead pigments with reference to Botticelli's Trionfo d'Amore. *Anal. Chim. Acta* 440:185-188

Spring, M. (2000) Occurrences of the Purple Pigment Fluorite on Paintings in the National Gallery. *National Gallery Technical Bulletin* 21:20-27

Spring, M. (2001) Pigments and color change in the paintings of Aelbert Cuyp. Aelbert Cuyp, exhib. Cat. National Gallery of Art, Ed. Wheelock Jr., A. K., Washington, 65-73

Spring, M. (2007-8) Pigments in sixteenth-century European painting, Making Art in Tudor Britain, Abstracts from Academic Workshops, National Gallery, London

Spring, M., Keith, L. (2009) Aelbert's Cuyt Large Dort: Colour Change and Conservation. *National Gallery Technical Bulletin* 30th Anniversary vol.

Srivastava, H., Lauer, H. V., Chase, L. L., Bron, W. E. (1971) Raman frequencies of fluorite crystals. *Phys. Lett.* 36A:333-334

Stege, H., Tilenschi, C., Unger, A. (2004) Known and unknown. New research in Vermeer's palette in the Procureur. In: Johannes Vermeer. Bei der Kupplerin. Eds. Neidhardt, U., Giebe, M., exhibition catalogue. [in German] Staatliche Kunstsammlungen Dresden, Dresden, 77-82

Šrein, V., Šreinová, B., Hradilová, J. (2010) Historical Exploitation of Fluorite as a Painting Pigment in Central Europe in the 15th - 16th Centuries. Proceedings of the 3rd Interdisciplinary Conference of ALMA held in Prague, 24-25 Nov, *Acta Artis Academica*: 213-225, Academy of Fine Arts in Prague, Prague

Švarcová, S., Hradil, D., Hradilová, J., Kočí, E., Bezdička, P. (2009) Microanalytical evidence of origin and degradation of copper pigments found in Bohemian Gothic murals. *Anal. Bioanal. Chem.* 395:2037-2050

Švarcová, S., Kočí, E., Bezdička, P., Hradil, D., Hradilová, J. (2010) Evaluation of laboratory powder X-ray micro-diffraction for applications in the fields of cultural heritage and forensic science. *Anal. Bioanal. Chem.* 398:1061-1076

Švarcová, S. (2011) Preparation, identification and degradation of copper-based inorganic painting pigments. Dissertation, Institute of Chemical Technology, Prague

Švarcová, S., Bezdička, P., Hradil, D., Hradilová, J., Žižak, I. (2011a) Clay pigment structure characterisation as a guide for provenance determination – a comparison between laboratory powder micro-XRD and synchrotron radiation XRD. *Anal. Bioanal. Chem.* 399:331-336

Švarcová, S., Klementová, M., Bezdička, P., Lasocha, W., Dušek, M., Hradil, D. (2011b) Synthesis and characterisation of single crystals of the layered copper hydroxide acetate $\text{Cu}_2(\text{OH})_3(\text{CH}_3\text{COO})\cdot\text{H}_2\text{O}$. *Cryst. Res. Technol.* 46:1051-1057

Švarcová, S., Bezdička, P., Hradil, D. (2012) Origin, Composition and Stability of Copper Pigments in Wall Paintings. Proceedings of the 4th Interdisciplinary Conference of ALMA held in Prague, 21-23 Nov, *Acta Artis Academica*: 213-225, Academy of Fine Arts in Prague, Prague

Thermo Scientific Nicolet iN10 FT-IR Microscope (2008) Thermo Fisher Scientific Inc., Waltham, MA, U.S.A. <https://static.thermoscientific.com/images/D12899~.pdf> Accessed 4 June 2013

Tien, P.-L., Waugh, T. C. (1969) Thermal and X-ray studies on earthy vivianite in Graneros shale (upper cretaceous), Kansas. *Am. Mineral.* 54:1355-1362

Uda, M. (2004) In situ characterization of ancient plaster and pigments on tomb walls in Egypt using energy dispersive X-ray diffraction and fluorescence. *Nucl. Instrum. Methods Phys. Res., Sect. B* 226:75-82

Van der Snickt, G., Dik, J., Cotte, M., Janssens, K., Jaroszewicz, J., De Nolf, W., Groenewegen, J., Van der Loeff, L. (2009) Characterization of a Degraded Cadmium Yellow (CdS) Pigment in an Oil Painting by Means of Synchrotron Radiation Based X-ray Techniques. *Anal. Chem.* 81:2600-2610

Van der Snickt, G., Miliani, C., Janssens, K., Brunetti, B. G., Romani, A., Rosi, F., Walter, P., Castaing, J., De Nolf, W., Klaassen, L., Labarque, I., Wittermann, R. (2011) Material analyses of 'Christ with singing and music-making Angels', a late 15th-C panel painting attributed to Hans Memling and assistants: Part I. non-invasive in situ investigations. *J. Anal. At. Spectrom.* 26:2216-2229

Van Eikema Hommes, M. (2004) Changing Pictures – Discoloration in 15th-17th-Century Oil Painting. Archetype Publications, London

van Loon, A. (2008) Color changes and chemical reactivity in seventeenth-century oil paintings. Dissertation, University of Amsterdam, Amsterdam

Vandenabeele, P., Lambert, K., Matthys, S., Schudel, W., Bergmans, A., Moens, L. (2005) In situ analysis of mediaeval wall paintings: a challenge for mobile Raman spectroscopy. *Anal. Bioanal. Chem.* 383:707-712

Vandenabeele, P., Garcia-Moreno, R., Mathis, F., Leterme, K., Van Elslande, E., Hocquet, F.-P., Rakkaa, S., Laboury, D., Moens, L., Strivay, D., Hartwig, M. (2009) Multi-disciplinary investigation of the tomb of Menna (TT69), Theban Necropolis, Egypt. *Spectrochim. Acta, Part A* 73:546-552

Vlček, V., Skála, R., Goliáš, V., Drahoukoupil, J., Čížek, J., Strnad, L., Ederová, J. (2012) Effect of natural irradiation in fluorites: possible implications for nuclear waste management? *J. Geosci.* 57:45-52

Westby, P.-P. (1974) The lining cycle: fundamental causes of deterioration in painting on canvas: materials and methods of impregnation and lining from the 17th century to the present day, Conference on Comparative Lining Techniques, Greenwich, 23-25 April 1974

Zachariasen, W. H. (2004) Theory of X-ray diffraction in crystals. Dover Publications, Mineola
Žák, T., Jirásková, Y. (2006) CONFIT: Mössbauer spectra fitting program, *Surf. Interface Anal.* 38:710-714

Želinská, J. (2012) Partial results of the research of the occurrence of fluorite in colour layers (study of the painting technique of Gothic wing altar). [in Slovak] *Proceedings of the Forum for conservationists-restorers*, Brno 2012, 18-27

APPENDIX A – PUBLISHED PAPERS

Čermáková, Z.*, Hradilová, J., Jehlička, J., Osterrothová, K., Massanek, A., Bezdička, P., Hradil, D. (2014a) Vivianite's identification in painted works of art and its significance for provenance and authorship studies. *Archaeometry* 56 (Suppl. 1): 148–167

Čermáková, Z.*, Bezdička, P., Němec, I., Hradilová, J., Šrein, V., Blažek, J., Hradil, D. (2014b) Naturally irradiated fluorite as a historic violet pigment: Raman spectroscopic and X-ray diffraction study. *Journal of Raman Spectroscopy*, In Press, DOI:10.1002/jrs.4627

Hradil D.* , Hradilová J., Bezdička P., Švarcová S., Čermáková Z., Košařová V., Němec I. (2014) Crocoite $PbCrO_4$ and mimetite $Pb_5(AsO_4)_3Cl$: rare minerals in highly degraded mediaeval murals in Northern Bohemia. *Journal of Raman Spectroscopy* 45(9):848-858

Švarcová S., Čermáková Z.*, Hradilová J., Bezdička P., Hradil D. (2014) Non-destructive micro-analytical differentiation of copper pigments in paint layers of works of art using laboratory-based techniques. *Spectrochimica Acta Part A: Molecular and Biomolecular Spectroscopy* 132: 514–525

Čermáková, Z.*, Švarcová, S., Hradilová, J., Bezdička, P., Lančok, A., Vašutová, V., Blažek, J., Hradil, D. (2014c) Temperature-related degradation and colour changes of historic paintings containing vivianite. *Spectrochimica Acta Part A: Molecular and Biomolecular Spectroscopy*, Accepted